Gut microbiota from patients with mild COVID-19 cause alterations in mice that resemble post-COVID syndrome

Viviani Mendes de Almeida
Laboratory of Microbiota and Immunomodulation - Department of Biochemistry and Immunology, Institute of Biological Sciences, Universidade Federal de Minas Gerais-UFMG, Belo Horizonte, MG, Brazil

Daiane F Engel
Department of Clinical Analysis, School of Pharmacy, Universidade Federal de Ouro Preto -UFOP, Ouro Preto, MG, Brazil

Mayra Fernanda Ricci
Laboratory of Microbiota and Immunomodulation - Department of Biochemistry and Immunology, Institute of Biological Sciences, Universidade Federal de Minas Gerais-UFMG, Belo Horizonte, MG, Brazil

Clênio Silva Cruz
Laboratory of Microbiota and Immunomodulation - Department of Biochemistry and Immunology, Institute of Biological Sciences, Universidade Federal de Minas Gerais-UFMG, Belo Horizonte, MG, Brazil

Icaro Santos Lopes
Laboratory of Virus Bioinformatics - Department of Biological Science, Center of Biotechnology and Genetics, Universidade Estadual de Santa Cruz-UESC, Ilhéus, BA, Brazil.

Daniele Almeida Alves
Laboratory of RNA interference and antiviral immunity - Department of Biochemistry and Immunology, Institute of Biological Sciences, Universidade Federal de Minas Gerais-UFMG, Belo Horizonte, MG, Braz

Mirna d' Auriol
Laboratory of Toxicology - Departament of Clinical and Toxicological Analysis, Faculty of Pharmacy, Universidade Federal de Minas Gerais-UFMG, Belo Horizonte, MG, Brazil

João Magalhães
Laboratory of Microbiota and Immunomodulation - Department of Biochemistry and Immunology, Institute of Biological Sciences, Universidade Federal de Minas Gerais-UFMG, Belo Horizonte, MG, Brazil

Giuliana S. Zuccoli
Laboratory of Neuroproteomics - Department of Biochemistry and Tissue Biology, Institute of Biology, State University of Campinas- UNICAMP, Campinas, SP, Brazil.

Bradley Joseph Smith
Laboratory of Neuroproteomics - Department of Biochemistry and Tissue Biology, Institute of Biology, State University of Campinas- UNICAMP, Campinas, SP, Brazil.

Victor Corasolla Carregari

Laboratory of Neuroproteomics - Department of Biochemistry and Tissue Biology, Institute of Biology, State University of Campinas- UNICAMP, Campinas, SP, Brazil.

Elayne Cristina Machado

Laboratory of Microbiota and Immunomodulation - Department of Biochemistry and Immunology, Institute of Biological Sciences, Universidade Federal de Minas Gerais-UFMG, Belo Horizonte, MG, Brazil

Victor M. Rocha

Laboratory of Microbiota and Immunomodulation - Department of Biochemistry and Immunology, Institute of Biological Sciences, Universidade Federal de Minas Gerais-UFMG, Belo Horizonte, MG, Brazil

Toniana G. Carvalho

Laboratory of Neurobiochemistry - Department of Biochemistry and Immunology, Institute of Biological Sciences, Federal University of Minas Gerais, Belo Horizonte, MG, Brazil.

Larisse de Souza Barbosa Lacerda

Center for Research and Development of Drugs - Department of Morphology, Institute of Biological Sciences, Universidade Federal de Minas Gerais-UFMG, Belo Horizonte, MG, Brazil

Jordane C. Pimenta

Center for Research and Development of Drugs - Department of Morphology, Institute of Biological Sciences, Universidade Federal de Minas Gerais-UFMG, Belo Horizonte, MG, Brazil

Izabela Galvão

Laboratory of Microbiota and Immunomodulation - Department of Biochemistry and Immunology, Institute of Biological Sciences, Universidade Federal de Minas Gerais-UFMG, Belo Horizonte, MG, Brazil

Mariana Aganetti Silva

Laboratory of Microbiota and Immunomodulation - Department of Biochemistry and Immunology, Institute of Biological Sciences, Universidade Federal de Minas Gerais-UFMG, Belo Horizonte, MG, Brazil

Erika da Silva Rosa

Laboratory of Microbiota and Immunomodulation - Department of Biochemistry and Immunology, Institute of Biological Sciences, Universidade Federal de Minas Gerais-UFMG, Belo Horizonte, MG, Brazil

Geovanni Dantas Cassali

Laboratory of Comparative Pathology - Department of Pathology, Universidade Federal de Minas Gerais-UFMG, Belo Horizonte, MG, Brazil.

Cristiana C. Garcia

Laboratory of Respiratory Viruses and Measles, Instituto Oswaldo Cruz, Fiocruz, Rio de Janeiro, RJ, Brazil

Mauro Martins Teixeira

Center for Research and Development of Drugs - Department of Morphology, Institute of Biological Sciences, Universidade Federal de Minas Gerais-UFMG, Belo Horizonte, MG, Brazil

Leiliane Coelho

Laboratory of Toxicology - Departament of Clinical and Toxicological Analysis, Faculty of Pharmacy, Universidade Federal de Minas Gerais-UFMG, Belo Horizonte, MG, Brazil

Fabiola Mara Ribeiro

Laboratory of Neurobiochemistry - Department of Biochemistry and Immunology, Institute of Biological Sciences, Federal University of Minas Gerais, Belo Horizonte, MG, Brazil.

Flaviano S. Martins

Laboratory of Biotherapeutic Agents - Department of Microbiology, Institute of Biological Sciences, Universidade Federal de Minas Gerais-UFMG, Belo Horizonte, MG, Brazil

Rafael Simone Saia

Laboratory of Intestinal Physiology - Department of Physiology, Ribeirão Preto Medical School, Universidade de São Paulo, Ribeirão Preto, SP, Brazil.

Vivian Vasconcelos Costa

Center for Research and Development of Drugs - Department of Morphology, Institute of Biological Sciences, Universidade Federal de Minas Gerais-UFMG, Belo Horizonte, MG, Brazil

Daniel Martins-de-Souza

Laboratory of Neuroproteomics - Department of Biochemistry and Tissue Biology, Institute of Biology, State University of Campinas- UNICAMP, Campinas, SP, Brazil.

João T. Marques

Laboratory of RNA interference and antiviral immunity - Department of Biochemistry and Immunology, Institute of Biological Sciences, Universidade Federal de Minas Gerais-UFMG, Belo Horizonte, MG, Braz

Eric R. G. R. Aguiar

Laboratory of Virus Bioinformatics - Department of Biological Science, Center of Biotechnology and Genetics, Universidade Estadual de Santa Cruz-UESC, Ilhéus, BA, Brazil.

Angelica T. Vieira (angelicathomazvieira@ufmg.br)

Laboratory of Microbiota and Immunomodulation - Department of Biochemistry and Immunology, Institute of Biological Sciences, Universidade Federal de Minas Gerais-UFMG, Belo Horizonte, MG, Brazil

---

Research Article

Keywords: COVID-19, SARS-CoV-2, Post-COVID, Microbiota, Inflammation, Antimicrobial-resistance, Gut-Lung-axis, Gut-Brain-axis

Posted Date: June 22nd, 2022

DOI: https://doi.org/10.21203/rs.3.rs-1756189/v1

Abstract

Background

There is mounting evidence that SARS-CoV-2 targets tissues beyond the respiratory tract. Long-term sequelae after COVID-19 are frequent and of major concern. Prolonged virus detection in the gut has been particularly intriguing. Of note, SARS-CoV-2 infection also disturbs the gut microbiota composition, a finding linked with disease severity in patients with COVID-19. Here, we aimed to characterize the functional role of the gut microbiota in the long-term consequences of COVID-19. To this end, we characterized the gut microbiota from COVID-19 human subjects and followed the effects of human fecal transfer to germ-free mice.

Results

The gut microbiota of post-COVID subjects (up to 4 months from the initial positive test) revealed a remarkable predominance of *Enterobacteriaceae* strains with multidrug-resistance phenotype compared to healthy controls. After fecal transfer to germ-free mice, animals receiving samples from post-COVID subjects displayed higher lung inflammation and increased susceptibility to pulmonary infection caused by an antimicrobial resistant *Klebsiella pneumoniae* strain. These mice also showed poorer cognitive performance associated with increased expression of TNF-α, reduced levels of brain-derived neurotrophic factor-BDNF and postsynaptic density protein-PSD-95 in the brain, as well as alterations of several biochemical pathways. These alterations were observed in the absence of SARS-CoV-2, suggesting that alterations in the gut microbiota caused them. Consistent with this hypothesis, brain dysfunctions induced in a mouse model of coronavirus infection were partially prevented by modulation of the microbiota via treatment with the commensal probiotic bacteria *Bifidobacterium longum* 5^{1A}.

Conclusions

Our results show prolonged impact of SARS-CoV-2 infection in the gut microbiota that persists even after the individuals have cleared the virus. Increased *Enterobacteriaceae* with antimicrobial resistance phenotype were of particular concern. Moreover, microbiota transfer from post-COVID subjects induced loss of brain cognitive functions and impaired lung defense in mice. Altogether, our work emphasizes the importance of microbiota as a target for therapies to help treat post-COVID sequelae.

Background

According to WHO, the severe acute respiratory syndrome coronavirus 2 (SARS-CoV-2) pandemic has claimed over 514 million confirmed cases and over six million deaths globally as of May 2022 [1]. Beyond the fatal short-term outcome, up to 75% of patients who had been hospitalized described persistent multi symptoms after the onset of coronavirus disease 2019 (COVID-19), including fatigue,

headache, and loss of memory, among others [2]. While the long-term complications of COVID-19 are common and increasingly recognized [3–5], the sequelae after clearance of the SARS-CoV-2 virus, especially in humans with mild or even asymptomatic COVID-19, remains unclear.

Although the newly emerged β-coronavirus, SARS-CoV-2, primarily infects the lung, the intestine is also vulnerable. The SARS-CoV-2 requires the angiotensin-converting enzyme 2 (ACE2) and Transmembrane Serine Protease 2 (TMPRSS2) as a receptor to enter the cells [6]. These receptors are not exclusively expressed in the lung but also, and even higher, in the gut [7, 8]. Moreover, the gut microbiota has been described as a factor that influences the COVID-19 severity and involves post-COVID long-term effects [9]. The human microbiota includes trillions of microorganisms, primarily bacteria, that inhabit our body, forming a complex and well-recognized ecosystem. An imbalance in the microbiota composition, named dysbiosis, is a major factor related to disease development [10, 11]. Moreover, viral infections can alter the gut microbiome composition resulting in the depletion of commensal microbiota leading to dysbiosis and impacting the host's gut homeostasis [9, 12, 13]. Individuals who experience severe COVID-19 have been shown to have a decrease in diversity and abundance in the commensal gut microbiota species and, consequently, an enrichment of opportunistic pathogens (independently of antibiotic treatment). These alterations were associated with the aberrant immune responses observed in COVID-19 patients [9, 14–18]. More recently, dysbiosis was described in the gut microbiota of individuals with long-COVID up to 6 months after their initial SARS-CoV-2 infection [2, 19]. This fact suggests that the long-term changes in the microbiota might support the symptoms of long-COVID, although there is no direct evidence for this link yet [17].

The gut microbiota can influence the immune system, lung, and brain functions *via* the gut–lung axis and the gut-brain axis, as well as other organs by different mechanisms: production of metabolites, miRNA, microbial-derived components (LPS, PSA), and others [20–25].

In recent years, the human gut microbiota environment has received increasing attention as a reservoir of antibiotic resistance genes, which disturbs the gut microbiota composition, and might be leading to the risk of infection due to multidrug-resistant bacteria [26, 27]. Indeed, during the COVID-19 pandemic, a "silent pandemic" of antimicrobial resistance (AMR) is gaining ground due to many factors, such as antimicrobial overuse, which requires urgent global action [28–31]. Many factors such as environment, diet, antibiotics, lifestyle, and infections can modulate human resistome, also contributing to the acquisition of resistance. Emerging evidence suggests that restoring the balance between gut microbiota microorganisms may be important to control the AMR threat and potentialize host immune response against pathogens [32]. More recently, a randomized clinical trial showed that daily use of *Lacticaseibacillus rhamnosus* GG probiotic protects against symptom development after exposure to SARS-CoV-2 [33]. However, few studies have been investigating the use of probiotics in controlling the human microbiota resistome [34, 35], and importantly, none on the impact on the gut microbiota of individuals with no/or mild symptoms of COVID-19.

Here, we investigated whether the gut microbiota derived from individuals infected with SARS-CoV-2 up to 4 months after initial infection and who had mild or no symptoms of COVID-19 at that time were associated directly with the post-COVID long-term consequences. To investigate this, we performed human fecal microbiota transference (FMT) to germ-free (GF) mice as an experimental approach. Our data provide evidence that gut microbiota drives important sequelae from SARS-CoV-2 infection demonstrated by the rise of AMR phenotype into human fecal microbiota, induction of lung inflammation affecting the host's lung bacterial infection defense, and brain dysfunction.

Methods

Study design

This cross-sectional study consisted of two steps: the first samples from human volunteers with or without COVID-19 were analyzed, and the second human feces from these volunteers were transplanted into germ-free mice (Fig.1). Initially, post-COVID and health volunteers (controls) were recruited, followed by the collection of feces and blood samples. Collections were performed from 1 to 4 months after infection (on average 2 months). The volunteers answered a survey consisting of clinical symptoms, medications used, and lifestyle questions. Samples were collected between October 2020 - April 2021 in Belo Horizonte metropolitan area in the state of Minas Gerais, Brazil. Fresh feces samples from the subjects were immediately used for Fecal Microbiota Transplantation (FMT) into Germ-Free mice (6-8 weeks old).

To investigate the effects of feces from post-COVID subjects on the susceptibility to pulmonary infection caused by a antimicrobial resistant bacteria, germ-free mice were infected with the bacteria *Klebsiella pneumoniae* afterfeces transfers from post-COVID and controls subjects. Animals wererandomly divided ten days after FMT into four groups: (1) Controls + Vehicle, (2) Controls + *K. pneumoniae* B31, (3) post-COVID + Vehicle and (4) post-COVID + *K. pneumoniae* B31. The infection with *K. pneumoniae* B31 was performed intratracheally. Subsequent analyses were performed 48 hours after infection. To evaluate the therapeutic effects of a probiotic bacterium, *Bifidobacterium longum* 5^{1A}, on post-COVID microbiota, mice were randomly divided into four groups: (1) Controls + Vehicle, (2) Controls + *B longum* 5^{1A}, (3) post-COVID + Vehicle, and (4) post-COVID + *B. longum* 5^{1A}. The *B. longum* 5^{1A} was administered through oral gavage every 48 hours for 12 days, until the end of the experiment and subsequent analysis.

Study subjects and sample collection

A total of 72 post-COVID subjects (1-4 months after SARS-CoV-2 infection) and 59 controls volunteers (SARS-CoV-2 negative test) were included in this study see the sample workflow in Additional File 1: FigS1.

Post-COVID subjects underwent SARS-CoV-2 testing (i.e., a nucleic acid amplification test [NAAT] or an antigen test) to confirm the infection. Those who tested positive for SARS-CoV-2 and did not show any symptoms related to COVID-19 were classified as asymptomatic. Clinical spectrum of disease severity

was classified according to the NHI COVID-19 Treatment Guidelines [34]. Control volunteers were included in the study if they never had symptoms related to COVID-19 and not tested positive for SARS-CoV-2. To ensure, serological tests were performed in all the volunteer serum samples to verify the presence or absence of SARS-CoV-2 antigens. The volunteers were instructed to self-collect the fecal sample in a sterile container and immediately store it in a home refrigerator (4^{o}C) within a maximum of 10 hours. The volunteers' sociodemographic characteristics, lifestyle, and health statuses are shown in Additional File 2: Table S1. All volunteers were aged between 15-60 years old. A survey was applied to investigate factors that influence the health and intestinal microbiota status of the subjects, such as comorbidities, eating habits, and antibiotics use at least 4 months before the application of the survey and sample collection. The parameters used to verify the eating habits of the volunteers are available in Additional File 3: Table S2. The exclusion criteria established in the present study were volunteers not having been vaccinated for SARS-CoV-2 and if they tested positive in the serological test performed on the day of sample collection.

Laboratory animals

Male and female Germ-Free Swiss/NIH mice derived from a GF nucleus (Taconic Farms, Germantown, USA), with ~8-weeks-old were used. They were maintained in flexible plastic isolators (Standard Safety Equipment Co., Pallatine, USA) using classical gnotobiology techniques [35] at the Gnotobiology Laboratory of the Federal University of Minas Gerais (UFMG), Minas Gerais, Brazil. Also, male and female C57BL/6J mice, aging ~8 weeks old, obtained from the UFMG animal facility, were kept in plastic cages in a room with controlled conditions (26°C, 12h light/dark cycle) with steam sterilized food (Nuvilab, Nuvital, Brazil) and water *ad libitum*. All mouse procedures were performed in accordance with guidelines from the Guide for the Care and Use of Laboratory Animals of the Brazilian National Council of Animal Experimentation (http://www.cobea.org.br/) and Brazilian Federal Law 11.794 (October 8, 2008). The animal study was reviewed and approved by The Institutional Committee for Animal Ethics of the Federal University of Minas Gerais (protocol nº CEUA/UFMG 281/2020 and 55/2021).

Human Fecal Microbiota Transplantation to GF mice

Fresh fecal samples were self-collected by volunteers, were weighed and resuspended in 0.9% sterile saline (NaCl) solution (100mg for each 1 mL of solution), homogenized, and kept for 10 minutes at 4 °C to big particles precipitate. For FMT, a single 100 µL aliquot of the supernatant was used for oral gavage of the GF mice. To assure stable human microbiota into GF mice after FMT 10 days have waited until the beginning of the experiments [36].

Klebsiella pneumoniae intratracheal infection

The bacterium used in the intratracheal pulmonary infection experiments was *K. pneumoniae* B31, a clinical isolate with a multidrug-resistance profile [37], gently provided by Prof. Vasco Ariston from the Laboratory of Cellular and Molecular Genetics at ICB/UFMG. For the procedure, animals were anesthetized intraperitoneally (i.p.) with 80 mg/kg ketamine and 10 mg/kg xylazine i.p., the trachea was exposed through a skin incision, and 25µL of the suspension containing 1×10^{6} CFU/mL of *K.*

pneumoniae B31, or sterile saline for mock controls, was injected with a 26-gauge needle [38]. After infection, the skin was sutured, and the mice were monitored for 2 days and then euthanized as described in the experimental design.

Mouse Hepatitis Virus-3 intranasal infection and virus quantification

The β-coronavirus mouse hepatitis virus MHV-3 was provided by Prof. Vivian Vasconcelos Costa and Prof. Mauro Martins Teixeira from the Center for Research and Development of Drugs at the Department of Morphology, UFMG. For intranasal infection, C57BL/6J mice were lightly anesthetized with 80 mg/kg ketamine and 10 mg/kg xylazine i.p., and received an intranasal inoculation of 30μL of a suspension containing 3×10^1 PFU of MHV-3 [39], or sterile saline for mock controls. Then, mice were monitored and euthanized 10 days after infection. MHV-3 was propagated in L929 cells, and viral titration was performed, as described previously [39]. RNA was extracted with kit QIAamp® Viral RNA for viral brain quantification, and the tissues were macerated in the first step with the lysis buffer. cDNA was synthesized using the kit iScript™ gDNA Clear cDNA Synthesis Kit (BIO-RAD), and qPCR assay was performed using Fast SYBR™ Green Master Mix (Applied Biosystems™). Primer sequences are described in Supplementary Information (Additional File 4: Table S3). The standard was obtained by extracting RNA from a known amount of PFU from MHV-3. Results of viral quantification were expressed in Arbitrary Units.

Treatment with *Bifidobacterium longum* 5^{1A} probiotic

The probiotic bacterium *B. longum* 5^{1A}, a strain isolated from the feces samples of healthy children [40] was provided by Prof. Flaviano S. Martins from the Laboratory of Biotherapeutic Agents at ICB/UFMG. *B. longum* 5^{1A} was cultured in De Man, Rogosa, and Sharpe (MRS) broth (Acumedia, USA) supplemented with 0.5% L-cysteine (Synth, Brazil) under an atmosphere containing 85% N_2, 10% H_2 and 5% CO_2, during 48h at 37°C in an anaerobic chamber (Forma Scientific, Marietta, GA, USA). Mice received by oral gavage, a single 100μL dose of suspension containing 1.0×10^9 CFU/mL, or sterile saline [38]. HM mice and C57BL/6 were treated every 48h, during 12 and 10 days, respectively.

Mouse behavioral tests

Novel object recognition and novel object location tests

Tests were performed in a 30 (w) x 30 (d) x 45 (h) cm arena. Before training, each animal was submitted to a 5 min habituation session the previous day, in which they were allowed to freely explore the empty arena. Training consisted of a 5 min session during which animals were placed at the center of the arena in the presence of two identical objects and the time spent exploring each object was recorded. Thirty minutes after training, animals were again placed in the arena for the test session, when one of the two objects used in the training session was replaced by a new one in the object recognition paradigm or moved to a new location in the new object location paradigm, and the time spent exploring familiar and novel objects (or object at the novel location) was measured [41]. The arena and objects were cleaned

thoroughly between trials with 70% ethanol to eliminate olfactory cues. Test objects were made of plastic [approximately 3 cm (w) x 3 cm (d) x 4cm (h)] and, during behavioral sessions were fixed to the arena floor using tape to prevent displacement caused by exploratory activity of the animals. Preliminary tests showed that none of the objects used in our experiments evoked innate preference by animals. Results were expressed as a percentage of time exploring each object or location (old or new) in relation to the total exploration time during the test session.

Bronchoalveolar lavage cell counts

After mice euthanasia, bronchoalveolar lavage (BAL) was collected by inserting 1mL of phosphate-buffered saline using 20-gauge catheter connected to a 1mL syringe into the lungs. The 1mL aliquot was collected, centrifuged, and resuspended in 100µL of sterile saline, and the total leukocytes were quantified by Neubauer chamber counting. In addition, differential counts were obtained from cytospin preparations [38].

Measuring SARS-CoV-2 load in the human feces

RNA extraction from feces samples was adapted from previously published protocols [42]. Briefly, fecal samples were diluted 1:5 (w:v) in guanidine, homogenized, and clarified by centrifugation at 4,000g for 20 min at 4°C. Viral RNA was purified using the QIAamp Viral RNA Mini Kit following the manufacturer's instructions, with a final elution volume of 50 µL.

Real-Time quantitative PCR (RT-qPCR) for SARS-CoV-2 test in feces samples and viral load quantification was performed on reactions with a final volume of 20 µL, using the one-step RT-qPCR Master Mix according to the CDC USA protocol [43]. The primers used for qPCR in the N1 and N2 regions of the nucleocapsid gene were sourced from Integrated DNA Technologies (cat. no. 10006770) that were manufactured using the U.S. CDC sequences and QC qualified under a U.S. CDC Emergency Use Authorization. For analysis, we adopted the amplification values of viral targets N1 or N2 with a threshold cycle (Ct) below 40.0 was considered positive for SARS-CoV-2, and above 40 as indeterminate or undetectable. This protocol was adapted from CDC 2019-Novel Coronavirus (2019-nCoV) Real-Time RT-PCR Diagnostic Panel Instructions. We used feces samples spiked with inactivated SARS-CoV-2 (stock titer 6.7 x 10^6 PFU/mL) as positive controls at different dilutions.

Inflammatory mediators' analysis by RT-qPCR in lung, intestine, and brain tissue from mice

Total RNA of the lung, intestine, and hippocampus from controls and post-COVID HM GF mice was extracted using TRIzol™ reagent (Thermo Scientific). cDNAs were prepared in a 20-µL final reverse transcription reaction and subjected to qPCR using the kit Power SYBR Green Master Mix (Applied Biosystems), following the manufacturer's instructions, in the QuantStudio™ 7 Flex real-time PCR system platform (Applied Biosystems). The primer sequences used are described in Supplementary Information (Additional file 4: Table S3). All RT-qPCRs showed good amplification quality, and gene expression changes were determined with the $2^{-\Delta Ct}$ method using Ribosomal protein L32 or normalization.

ELISA for measurements of Intestinal fatty acid-binding protein (I-FABP) and cytokines

ELISA techniques were used to quantify the concentrations of I-FABP as described before [44]. IL-10, TNF-a and IL-1b concentrations were determined using IL-10 ELISA kits (R&D Systems, USA) according to the manufacturer's instructions. The analyses were performed in duplicate.

Short-chain fatty acids (SCFAs) measurement

The SCFAs measurements were performed as previously described, with adaptations [45]. Feces samples were suspended in 1% phosphoric acid (1:6 – W: V) (Merck, USA), vortexed, and centrifuged at 20,000g for 30 min at 4°C. The supernatant was filtered through a cellulose acetate membrane (0.22 µm), and 10 µL were injected directly into HPLC, using an ionic exchange resin column 300×7.8 mm (Sigma, Germany) with a Micro-Guard cation H^+ cartridge (Sigma, Germany) and detector set at 210 nm. The flow rate was 0.5 mL/min until 35 minutes of chromatographic run, being changed to 0.7 mL/min until the end of the run. The column temperature was 30ºC. For serum samples, the SCFAs measurements were performed as previously described, with adaptations [46]. Serum samples were suspended in formic acid 1 $mol.L^{-1}$, and solution of the internal standard, 2-ethyl-butyric acid 1 $mol.L^{-1}$ (Sigma, Germany) was added, in proportions 5:5:1 respectively. Then, the suspension was vortexed and centrifuged at 12,000 g for 30 min at 4°C. After, 2 µL of the supernatant were injected into Gas Chromatograph–FID (Agilent, USA), using HP-FFAP column 19091F-105 (Agilent, USA), 50m×0.20mm×0.33 µm, and the detector was set in 240°C. The chromatographic conditions were 60°C for 0.5 minutes, heating at $8°C.min^{-1}$ to 180°C for 1 minute. New heating rate from 20 $°C.min^{-1}$ to 240 °C for 7 minutes. The total run time was 26.5 minutes. Seven-point external calibration curves were adopted to quantify fecal and serum samples, using analytical grade SCFA (Sigma, Germany) as standards.

Histopathology and immunohistochemistry analysis

Intestine and lung tissue from HM GF mice were collected and processed. The inflammatory score was performed with hematoxylin and eosin (H&E) stained slides and evaluated airway, vascular and parenchymal inflammation [47,48]. For immunohistochemistry analysis, lung tissue slides from controls, and post-COVID HM GF mice were immune-stained as described before [49]. Briefly, the slides were incubated with primary anti-α-actin antibodies (human, 1:500) (DAKO, USA) overnight at 4ºC. Then, the primary antibodies were detected using an anti-mouse/anti-rabbit detection system (Novolink Polymer Detection System; Leica Biosystems, Newcastle Upon Tyne, UK) according to the manufacturer's instructions. The sections were counterstained in diluted Harris Hematoxylin solution and permanently mounted with Entellan (Merck, USA). For the morphometric analysis, images (20X objective) were acquired from α-actin immunolabeled to quantify the muscle layer of the lung section using the Image J1.52 program (NIH, USA). All the analyzes were examined under a light microscope by a pathologist who was blinded to the experiment.

Cultivable fecal microbiota quantification

Fresh fecal samples were weighed, homogenized in sterile 0.9% saline (100mg for each 1 mL of saline), and serially diluted (1:10). Subsequently, different dilutions were plated on different selective media (Merck, USA) for quantification of total aerobic (blood agar in aerobiosis) and anaerobic bacteria (blood agar supplemented with hemin (5 µg/mL) and menadione (1 µg/mL) in anaerobiosis), *Enterobacteriaceae* (MacConkey agar in aerobiosis), *Staphylococcus* (Salt Mannitol agar in aerobiosis), *Bacteroides* (Bacteroides Bile Esculin agar in anaerobiosis), Acid Lactic Bacteria (De Man, Rogosa and Sharpe in aerobiosis) and *Bifidobacterium* and anaerobic Lactic Acid Bacteria(De Man, Rogosa and Sharpe in anaerobiosis) populations. Aerobic plates were incubated for 24h at 37°C under standard conditions. Anaerobic plates were incubated in an anaerobic chamber (Forma Scientific, Marietta, GA, USA) under an atmosphere containing 85% N2, 10% H2, and 5% CO2 at 37°C for up to 72h. After incubation, the colonies were counted, and data were expressed as the $\log_{10}$ of colony-forming units (CFU) per gram of feces.

Quantification of *Enterobacteriaceae* on bronchoalveolar lavage

The BAL samples were directly plated on MacConkey agar, incubated in aerobic conditions, and kept under the same culture conditions mentioned above. After incubation, the colonies were counted, and data were expressed as the $\log_{10}$ of CFU per mL of BAL.

Enterobacteriaceae antimicrobial resistance test and identification

After fecal microbiota cultivation, individual *Enterobacteriaceae* colonies with different morphologies were isolated from MacConkey medium (Sigma, Germany) plates. Pure colonies were suspended in sterile 0.9% saline at a $1.5x10^8$ CFU/mL concentration according to the 0.5 McFarland standard. Then, a sterile swab was soaked in the bacterium solution and inoculated by spreading on Mueller Hinton Agar plates (140x15mm) (Merck, USA). After 15 minutes, a dispenser (Thermo Scientific™ Remel™) with 12 discs (Thermo Scientific™ Oxoid™) referring to β-lactam (amoxicillin-clavulanic acid, cephalosporin, ertapenem, meropenem, imipenem), aminoglycosides (amikacin, streptomycin, gentamicin), quinolones (ciprofloxacin, levofloxacin, norfloxacin), sulfonamide and folate inhibitors (sulfamethoxazole-trimethoprim) and macrolides (azithromycin) antibiotics were added to the inoculated plates. The plates were incubated at 37°C for 24h. The presence or absence of bacterial growth inhibition zones was observed and measured to determine the resistance profile in: sensitive, intermediate, or resistant, according to the CLSI M100Ed31 guidelines. The resistance phenotype was determined according to the number of antimicrobials classes in which each strain presented resistance, being resistant (1-2 antimicrobials) or multidrug-resistant (≥3 antimicrobials). Identification of *Enterobacteriaceae* strains was performed by Matrix Associated Laser Desorption-Ionization - Time of Flight (MALDI-TOF), using the FlexControl MicroFlex LT mass spectrometer (Brunker Daltonics) as described before [50]. Before identification, calibration was done with the bacteria *Escherichia coli* DH5α test standard (Brunker Daltonics). For the construction of the network, data from bacteria that showed resistance to ≥2 antimicrobials classes were used. Nodes were classified as the isolated bacteria and edges as shared AMR phenotype. The network was non-directional, and the nodes color was determined according to the

resistance phenotypeof the antimicrobial classes. Node size was established according to the number of antimicrobial classes to which each bacterium was resistant. Edge weight was defined according to the number of resistance classesthat the bacteria shared with each other. Network co-occurrence analysis, visualization, and property measurements were performed using the platform Gephi [51].

LC-MS/MS Analysis

Hippocampus samples were mechanically lysed with an ultrasonication probe in protein extraction buffer (100 mM Tris-HCl, 1 mM EDTA, 150 mM NaCl, 1% Triton-X) and protease inhibitors cocktail (Protease Inhibitor Cocktail, SIGMA). 20 µg of protein were submitted to the FASP protocol for tryptic digestion [52]. Digested peptides were then resuspended in 0.1% formic acid and fractionated on an ACQUITY MClass System (Waters Corporation). 1 µg of digested samples were individually loaded onto a Symmetry C18 5 µm, 180 µm × 20 mm precolumn (Waters Corp.) and subsequently separated in a 120 min reversed phase gradient at 300 nL/min (linear gradient, 3–55% ACN over 90 min) using an HSS T3 C18 1.8 µm, 75 µm × 150 mm nanoscale and LC column (Waters Corp.) maintained at 30 °C. For the gradient elution, water-formic acid (99.9/0.1, v/v) was used as eluent A and acetonitrile formic acid (99.9/0.1, v/v) as eluent B. Separated peptides were analyzed in a Synapt G2-Si mass spectrometer directly coupled to the UPLC system. Mass spectrometry was conducted using data-independent acquisition (DIA) in expression mode (MSe), switching between low (4 eV) and high (25–60 eV) collision energies on the gas cell, using a scan time of 1.0s per function over 50–2000 m/z. All spectra were acquired in ion mobility mode (wave velocity: 1.000m/s and a transfer wave velocity: 75m/s). A reference lock mass ([Glu1]-Fibrinopeptide B Standard, Waters Corp.) has been employed for online calibration. Experiments were performed in technical triplicates. LC-MS/MS data were processed for qualitative and quantitative analysis using the software Progenesis (Waters Corp.). Protein identification was obtained using *Mus musculus* database (UniProt KB/Swiss-Prot Protein reviewed). Search parameters were set as: automatic tolerance for precursor ions and product ions, minimum 1 fragment ions matched per peptide, minimum 3 fragment ions matched per protein, minimum 1 unique peptide matched per protein, 2 missed cleavage, cysteine carbamidomethylating as fixed modification, and oxidation of methionine as variable modifications, false discovery rate (FDR) of the identification algorithm < 1%. Label free quantitative analysis was obtained using the relative abundance intensity integrated in Progenesis software, using all peptides identified for normalization. Filtered tables were generated to exclude proteins with no statistical significance according to ANOVA ≥ 0.05. In silico systems biology was performed using DAVID Bioinformatics Resources [53].

Fecal DNA extraction and sequencing

Feces samples self-collected by the volunteers were stored in a freezer at −70 °C. DNA extractions were performed using a QIAamp DNA Stool Mini Kit (Qiagen, USA) according to the manufacturer's instructions. Then, DNA quality was checked by 1% (w/v) agarose gel electrophoresis and quantified by NanoDrop™ 2000/2000c Spectrophotometer (Thermo Scientific™). DNA was used as a template in PCR amplicon targeting the V3 and V4 hypervariable regions of the bacterial 16S rRNA gene. The Illumina 16S

Metagenomic Sequencing Library Preparation protocol was used to prepare the 16S metagenomics library and sequencing (Illumina, USA). PCR amplification protocols, adapter primers, index sequences, and PCR clean-up process were performed as described in the protocol [54].The 16S library was quantified by Qubit dsDNA HS Assay Kit (Invitrogen, USA) and checked with a 2100 Bioanalyzer Instrument (Agilent Technologies, USA). The sample pool (4 nM) library was diluted further final concentration of 8 pM and added to 20% (v/v) of 8 pM PhiX DNA (Illumina, USA), following Illumina guidelines. Sequencing was performed using the Miseq reagent kit v3 (600 cycles) in the Illumina MiSeq platform and 2×300 bp (MSC v2.4) according to the manufacturer's instructions (Illumina, USA).

Sequence data processing, inferring gut microbiota composition, and statistical analysis

Processing of metagenomic sequencing data was performed using QIIME2 pipeline [55]. First, sequenced reads were denoised with DADA2 and then processed by VSEARCH [56] to filter eventual chimeras and perform *de novo* clustering of valid sequences into OTUs requiring 97% sequence similarity. Next, MAFFT Fasttree was applied to conduct phylogenetic analysis based on OTUs. α- and β-diversity were analyzed using the core-metrics-phylogenetic method built-in on QIIME2: for the α-diversity, were calculated Shannon's diversity index and Chao1; for β-diversity, were calculated Bray-Curtis and weighted UniFrac distances. OTUs were taxonomically classified using Naive Bayes classifiers trained with Silva v. 138, setting 97% of sequence similarity for full-length OTUs [57]. Differential abundance was calculated using ANCOM [57]. The metagenomic libraries produced in this work were deposited in the NCBI SRA database under project number PRJNA843134.

Statistical analysis

Statistical analyses and graphs were done using GraphPad Prism7 (GraphPad Software, La Jolla, CA, United States). Data are shown as mean ± standard deviation (SD). Data that presented normal distributions ($p > 0.05$ by Shapiro–Wilk tests) were evaluated by Student's *t*-test, one-way and two-way analysis of variance (ANOVA), depending on the experimental design. Following significant ANOVAs, we performed a post-hoc test according to the coefficient of variation (CV): Tukey (CV ≤ 15%), Student's Newman-Keuls (CV entre 15 - 30%) e Duncan (CV >30%). Data from object recognition and location tests were expressed as exploration percentage and analyzed by one-sample *t*-tests to determine whether the percentage of the exploration differed from the chance performance of 50%. The differences were considered significant when $p < 0.05$. Outliers were only excluded following Grubbs' test and indicated in figure legends.

Results

Comparison of clinical, dietary, and microbiological parameters between controls (non-COVID) and post-COVID volunteers

Clinical characteristics of all subjects were summarized in Additional File 2: Table S1. 54% of all volunteers (n=72) were post-COVID subjects, with 6.1% (n=8), 42% (n=55) and 6.9% (n=9) classified as

asymptomatic, mild, and moderate disease, respectively (Additional File 2: Table S1). Controls and post-COVID subjects with preexisting comorbidities presented hypertension, hypothyroidism, irritable bowel disease, and chronic respiratory diseases (Fig. 2A). Preexisting comorbidities were similar between controls and post-COVID subjects. The dietary score was also similar between the two groups, showing a similar eating profile (Fig. 2B). Gastrointestinal symptoms appeared in 48.4% (n=31) of the post-COVID subjects (Additional File 2: Table S1). Furthermore, 35.5% (n=22) of the post-COVID subjects used antibiotics during the SARS-CoV-2 prodromal and transmission states and at least 3 months before applying the survey (Fig. 2C). All fecal samples tested negative for the presence of SARS-CoV-2 nucleic acid by RT-qPCR at the time of collection (Fig. 2D).

Gut microbiota composition by 16S sequencing was analyzed in 44 fecal samples due budget constraints. However, we attempted to sample paired subjects from the same family. However, because human-associated microbiota communities vary across individuals but cohabiting family members share microbiota with one another [58,59], we prioritized sampling paired feces from family members living in the same household, that one had SARS-CoV-2 infection (post-COVID) (n=11) and the other did not (controls) (n=11). For the 16S sequencing, an additional 11 controls and 11 post-COVID feces samples were chosen randomly. Detailed, taxonomic composition analysis of the gut microbiota revealed a similar profile between individual samples from controls and post-COVID subjects (Fig. 2E). β-diversity metrics, based on weighted UniFrac distances, showed no significant differences in the gut microbiota between post-COVID and control subjects (Fig. 2F). Comparison of the α-diversity indexes, Shannon, Simpson, and Chao1, also confirmed similar taxonomic diversity between controls and post-COVID subjects (Fig. 2G).

To explore the prolonged impact of COVID-19 on the gut microbiota functionality, we analyzed the concentration of gut microbiota-derived metabolites by measuring SCFAs in fecal samples using high-performance liquid chromatography (HPLC). To avoid the inter-individual differences between microbiota composition and microbial products, since their are highly variable components between humans [60], we decided to focus our analyses on controls and post-COVID subjects living in the same household. This strategy was performed to minimize other contributions to microbiota variations and better limit the observations to the remained impact of SARS-CoV-2 on the gut microbiota. Thus, fecal samples harvested from controls and post-COVID members belonging to the same family (n=11 families) were preferentially used for this analysis (Fig. 2H). We noted significant differences in propionate levels and reduced levels of acetate and butyrate in the feces of post-COVID subjects compared to controls, although we did not find statistical significance (Fig. 2H). Altogether, these findings suggest that SARS-CoV-2 infection affects the gut microbiota metabolism even though no major alteration in the composition of the gut microbiota in post-COVID subjects compared to controls was observed.

Prevalence of antimicrobial-resistant bacteria in gut microbiota from post-COVID humans

To evaluate the relationship between the COVID-19 pandemic and the spread of AMR, we investigated antimicrobial-resistantin cultivable fecal *Enterobacteriaceae* strains from controls and post-COVID subjects (Fig. 3A). *Enterobacteriaceae* family was chosen for the analysis due to its importance as

pathobionts that carry and transmit AMR genes of clinic interest. Co-occurrence network analysis of *Enterobacteriaceae* strains isolated from the gut microbiota of controls (n=57) and post-COVID (n=53) subjects revealed structural differences associated with AMR (Fig. 3B). The microbiota of controls and post-COVID subjects was characterized by three interconnected communities of bacteria based on the AMR profile with common resistance phenotypes to aminoglycosides, sulfonamides, quinolones, and cephalosporins. Controls subjects had fewer and lesser connected AMR bacteria (nodes = 35, edges = 238) than those (nodes = 51, edges = 759) from post-COVID. Notably, control and post-COVID subjects differentiated in the resistance to β-lactams and penicillin's antibiotics (Fig. 3B). This was also observed when we analyzed the cultivable *Enterobacteriaceae* population analysis. Overall, these results indicate a higher level of AMR in the *Enterobacteriaceae* family isolated from post-COVID subjects. Despite similar CFU numbers between the two groups (Fig. 3C), post-COVID subjects presented a higher percentage of strains with a drug-resistant (45% DR) and multidrug-resistant (23% MDR) phenotype when compared to controls (39% DR and 13% MDR) (Fig. 3D). Moreover, we found increased *Klebsiella sp.*and reduced AMR *Escherichia sp.* in the microbiota of post-COVID subjects compared to controls (Fig. 3E). Of note, MDR *Klebsiella sp.* did not appear altered between the groups (data not shown). Together, our results indicate an increase in AMR *Enterobacteriaceae* in the gut microbiota of post-COVID individuals. These changes in the microbiota community after SARS-CoV-2 infection led to increased AMR in the *Enterobacteriaceae* community.

Signs of altered intestinal homeostasis in post-COVID subjects

We next decided to investigate factors regulating intestinal homeostasis that could influence systemic inflammation. For this analysis, blood samples collected from controls and post-COVID members belonging to the same family (n=11 families) were preferentially used (Fig. 4A). We observed similar LPS levels in the serum of controls and post-COVID subjects (Fig. 4B), suggesting no difference in translocation of bacteria from the gut. In contrast, we observed higher levels of I-FABP, a marker for epithelial damage, and lower levels of IL-10, an anti-inflammatory cytokine, in the serum of post-COVID subjects compared to controls (Fig. 4C-D). In contrast, we observed no significant differences in pro-inflammatory cytokines, including TNF-a and IL-1b (Fig. 4E-F). These findings suggest that post-COVID subjects had signs of intestinal epithelial injury due to increased circulating I-FABP levels even though no strong marker of systemic inflammation was observed.

Post-COVID gut microbiota induces physiological alterations in the lung of GF mice and impairs defenses against bacterial infections

To gain an understanding of the contribution of post-COVID microbiota to the host, we performed human fecal microbiota transference in germ-free mice. To employ a rigorous experimental approach to generate humanized microbiota associated mice, feces samples harvested from controls and post-COVID members belonging to the same family were prioritized (Fig. 5A). After the fecal microbiota transference to germ-free, mice were housed and waited for 10 to stabilize and colonize the human-derived microbiota. Humanized microbiota (HM) mice receiving fecal transfer from post-COVID subjects' donors did not show

intestinal structural changes compared to controls (Additional File 5: Figure S2 B-C), but the colon exhibited signs of Peyer's patch activation (Additional File 5: Figure S2 C–D). Circulating LPS levels were also found at similar concentrations among controls and post-COVID HM mice (Additional File 5: Figure S2 E). Consistent with results from the direct analysis of fecal samples from subjects, we did not observe differences between the fecal cultivable microbiota from mice receiving samples from controls and post-COVID subjects (Additional File 5: Figure S2 F). However, we observed the β-diversity analysis revealed significant differences between controls and post-COVID recipient mice, although no significant differences were observed in taxonomic composition and α-diversity indexes (Additional File 5: Figure S2 G-I)

To explore the impact of post-Covid microbiota in extra-intestinal organs, we also analyzed the effect of fecal transfer on lung inflammation and the response to infections. By conventional H&E staining, we observed foci of inflammatory infiltrate in the perivascular and peri-bronchial regions with an increased score in post-COVID HM mice compared to controls (Fig. 5B top panels, and E). There was no detection of SARS-CoV-2 nucleic acid in lung tissues (Fig. 5C), which corroborates the absence of virus in fecal samples used for the initial transfer (Fig. 2E). We also observed an increase in inflammatory cells on bronchoalveolar fluid (BAL) of post-COVID HM mice compared to the controls (Fig. 5D). Moreover, we observed a significant increase in the expression of α-smooth muscle actin (α-SMA) by immunohistochemical analysis in post-COVID HM mice compared to the controls (Fig. 5B bottom panels, and F). Our data indicate that transfer of post-COVID subjects fecal samples affected the lung of recipient mice in the absence of SARS-CoV-2, suggesting the alterations in the intestinal microbiota caused by COVID-19 can directly impact lung inflammation.

To further explore the consequences of the lung alterations induced by the post-COVID FMT observed in HM germ-free mice, we further investigated the influence of post-COVID microbiota on a lung infection caused by an AMR *K. pneumoniae* (B31 strain) (Fig. 5A). We first observed that the histopathological score was higher in *Kp*-infection mice than vehicle-treated mice in both post-COVID and controls (Fig. 5H). We observed intense inflammatory cells infiltration in the lungs of post-COVID HM mice infected with *K. pneumoniae* B31 *(Kp)*, associated with significant pathological changes in the perivascular, peri-bronchial, and parenchyma associated with emphysema areas in the lung compared to the controls *Kp*-infected (Fig. 5G). We detected an increase in inflammatory cells and higher levels of *Enterobacteriaceae* on the BAL from post-COVID *Kp*-infected HM mice compared to controls (Fig. 5I-J).

These results suggest that post-COVID microbiota was able to exacerbate the pulmonary inflammatory condition and cause higher lung tissue damage in response to infection by the multiresistant *K. pneumoniae* B31 strain. We also performed an FMT experiment with frozen feces (Additional File 6: Figure S3A) and observed a similar although less strong phenotype in HM mice that received samples from post-COVID subjects compared to controls (Additional File 6: Figure S3 B-E). This difference may be explained by a decrease in cultivable microbial abundance and diversity when we utilized frozen feces (Additional File 6: Figure S3 F).

Post-COVID human gut microbiota induces memory impairment and changes in the hippocampus of mice

Post-COVID sequalae are commonly associated with brain dysfunction. To evaluate the impacts of fecal transfer from post-COVID subjects on brain functions, we performed an experiment using GF mice. Animals that received feces of controls or post-COVID subjects were submitted to different cognitive tests (Fig. 6A). GF mice that received feces from post-COVID subjects showed memory impairment in the recognition and location tests compared to controls (Fig. 6B). Mice receiving post-COVID feces showed increased expression of the pro-inflammatory cytokine *tnf* and lower levels of neuroprotective factors *bdnf* and *psd*-95 in the hippocampus (Fig. 6C-E). *B. longum* 5^{1A}treatment of mice receiving feces from post-COVID subjects partially prevented these alterations in gene expression, although we did not find statistical differences (Fig. 6C-E). These mice did not perform significantly different than animals treated with the vehicle on the recognition and location test, albeit there was also a tendency for some animals to perform better (Fig. 6F).

In order to understand how the fecal transfer from post-COVID patients could impact memory in mice, we analyzed the proteome of the hippocampus from GF mice following the FMT protocol. We compared animals that received feces from controls or post-COVID subjects (Fig. 6G). We also compared GF mice that received feces from post-COVID subjects along with vehicle or the probiotic *B. longum* 5^{1A}treatment (Fig. 6H). A total of 1461 proteins were identified and quantified. When compared to controls, 359 were differentially expressed proteins in the hippocampus of mice receiving feces from post-COVID subjects. Gene ontology analysis of differentially expressed proteins indicated that receiving feces from post-COVID subjects affected several biological pathways associated with neuronal synapsis, such as protein transport, exocytosis, vesicle transport and docking (Fig 6I). Transfer of feces from post-COVID subjects also affected antigen processing and presentation, protein transport and secretion, vesicle docking involved in exocytosis, NADH metabolic process, carbohydrate metabolic process, microtubule cytoskeleton organization, GTP binding, GTPase activity, and nucleotide-binding. Treatment with *B. longum* 5^{1A}did not have a significant effecton the hippocampus proteome affecting only the expression of 89 proteins when compared to vehicle control. Gene ontology analysis suggested minor effects on necroptosis, multicellular organism development, chromatin silencing, late endosome membrane, and GTPase activator activity. For details regarding pathways and proteins, see Additional File 7-10: Table S4-7.

Microbiota modulation protects from cognitive impairment in a murine model of coronavirus infection

Our results suggest that changes in the gut microbiota might be associated with the cognitive dysfunction of coronavirus infection. To access the direct impact of microbiota modulation during coronavirus infection, we used an experimental murine model with mouse hepatic virus (MHV) -3, a β-coronavirus (Additional File 11: Figure S4 A). In this model, we demonstrated that infected animals showed memory impairment using the object location test, which was prevented by pre-treatment with the probiotic *B. longum* 5^{1A} (Additional File 11: Figure S4 A-B). Interestingly, similar levels of MHV-3 were

found in the brain of infected mice treated or not with *B. longum* 5^{1A} (Additional File 11: Figure S4C). Of note, the same levels of cultivable *Bifidobacterium* were present in mice feces even after treatment with *B. longum* 5^{1A}(data do not show). However, fecal lactic acid bacteria levels were higher in MHV-3 infected animals treated with the probiotic (Additional File 11: Figure S4D). Therefore, these findings demonstrate that a murine model of infection by a β-coronavirusalso produces memory impairment, which can be prevented by treatment with a probiotic and modulation of the gut microbiota.

Altogether, the data indicate that the gut microbiota, both immediate and during post-infection, observed respectively in the MHV-3 model and post-COVID FMT, is an important player to disrupt hippocampal function and lead to cognitive impairment.

Discussion

Among the pathophysiological responses triggered by SARS-CoV-2 infection, several studies have demonstrated gastrointestinal symptoms and alterations in the gut microbiota associated with COVID-19 [19, 61, 62]. However, these studies have primarily identified associations between microbiota components and COVID-19 manifestations. Here, we showed an increase in AMR bacteria and changes in metabolic profile in the gut microbiota of post-COVID subjects. Moreover, after fecal transfer to germ-free mice, we observed lung and brain dysfunction in animals receiving feces from post-COVID donors, pointing to a direct functional connection between the gut microbiota and some disease manifestations.

Our study is the first to show alterations in the gut microbiota associated with an increase of AMR *Enterobacteriaceae* in post-COVID subjects. Interestingly, we did not expect significant changes since our subjects were asymptomatic or had mild COVID-19 symptoms. During COVID-19, the uncontrolled and indiscriminate use of antimicrobials associated with the absence of effective drugs may explain the exacerbation AMR threat [63–70]. However, our post-COVID subject group did not report higher antibiotic use compared to controls which raises concerns of a “silent” spread of antimicrobial resistance in the environment. Our findings draw attention to the importance of COVID-19 in the AMR spread even in mild and moderate cases, since these conditions account for the majority of COVID-19 cases worldwide [1]. We found a predominant increase of AMR *Klebsiella sp.* in the gut microbiota of post-COVID subjects. This bacterium belongs to the ESKAPE group of antimicrobial-resistant bacteria and has been reported to be responsible for most nosocomial pneumonia infections caused in hospitalized patients with COVID-19 [71–74]. Of note, mice receiving a fecal transfer from post-COVID donors presented worse lung injury after infection with *K. pneumoniae* reinforcing the connection between gut and lung [75, 76]. Thus, modulation of the gut microbiota may be used as a strategy to prevent or improve host defense against bacteria in the lung.

We found an increase of cultivable *Enterobacteriaceae* in the lung of mice that received a fecal transfer from post-COVID donors, which was not observed in controls. This lung incremental colonization of LPS-producing bacterial could compromise the lung defenses against bacteria. We found no differences in systemic levels of LPS between controls and post-COVID humanized microbiota mice, which we

attributed to the fact that quantification of LPS can be intricate and variable, as already reported [77]. Additionally, direct dysbiosis of the lung microbiota can help explain lung dysfunction, although we did not investigate the lung microbiome [78]. The connection between gut and brain is often discussed [79, 80], but the lung-brain axis has only recently been considered [81, 82]. Although our study has not assessed the role of the lung microbiota in neurological disorders, clinical studies have found differences in the lung microbiota when comparing control and cognitively impaired individuals [83, 84]. Previous studies have suggested that even minimal alterations in the lung microbiome were enough to affect the central nervous system, while major changes in gut microbiome were necessary [85]. Thus, lung alterations induced by the post-COVID microbiota in humanized microbiota mice might be associated with neurological outcomes. Our findings that the post-COVID microbiota can induce memory impairment in humanized microbiota mice are in accordance with the neurological outcomes in post-acute COVID in humans [86, 87].

Production of metabolites, particularly SCFAs, by the gut microbiota is a major mechanism that explains the gut-lung and gut-brain connections [20, 88]. We found reduced levels of SCFAs, mostly propionate, in fecal samples from post-COVID donors, which may affect the gut-brain connection and help explain the neurological sequelae observed in post-acute COVID. Propionate has been shown to modulate blood-brain barrier integrity and the inflammatory response in microglia [85]. In line with our findings, decreased SCFA levels were associated with Alzheimer's disease in clinical studies and experimental models [89–91]. Biological effects of SCFAs are triggered mainly by direct binding to specific G-protein coupled receptors (GPCRs), such as GPR41 and GPR43, which are expressed in both peripheral and central nervous system [92, 93]. We also observed clear differences in the systemic levels of host factors, such as I-FABP and IL-10, indicating the loss in intestinal homeostasis in post-COVID subjects compared to controls. Indeed, I-FABP has been shown to be a relevant biomarker for COVID-19 disease prognostic [44].

Interestingly, our proteome analysis also indicated alterations in several GPCRs signaling (GTP binding and GTPase activity) in the hippocampus of humanized microbiota mice that received post-COVID fecal transference. This supports the hypothesis that gut-produced metabolites, such as SCFAs, might be important players in the brain dysfunction observed in our model. Besides the direct effect of the gut microbiota-produced metabolites [80, 85, 94] on the central nervous system, other chemicals, neuronal and immunological factors may also be involved in hippocampus dysfunction [80]. Here we observed increased TNF-α expression in the hippocampus of mice that received a fecal transfer from post-COVID donors, indicating that a neuroinflammatory response might have been triggered in the central nervous system. A similar effect has been described in a colitis model, where systemic driven TNF-α hippocampal expression was associated with memory impairment, which was abolished upon restoration of the gut microbiota [95, 96]. In our study, there was a reduction in the expression of the neuroplasticity markers BDNF and PSD-95 in the hippocampus of post-COVID humanized microbiota mice. This impairment in neuroplasticity was previously observed when FMT from transgenic Alzheimer's disease mice transferred their cognitive phenotype to the recipient mice [97, 98]. By using a probiotic to assess if strategies of gut microbiota modulation would counteract the brain dysfunction associated with post-COVID sequela, we found mild beneficial effects in changes in gene expression of TNF-α, BDNF, and PSD-95 in the

hippocampus of human post-COVID FMT mice. The particularity of the probiotic *B. longum* 5^{1A} strain is the ability to produce high levels of SCFAs, which has beneficial effects in controlling host inflammation, particularly in the lung [38, 40, 99]. Conversely, we found enrichment of Necroptosis-related pathways in the post-COVID humanized microbiota vehicle mice that were reduced in post-COVID humanized microbiota probiotic-treated mice. This result might be associated with the effect of the probiotic counteracting the increase in TNF-α expression since this cytokine triggers this kind of neuronal cell death [100, 101]. Accordingly, with these data, we also observed a neuroprotective effect of *B. longum* that prevented memory impairment induced in a murine model of coronavirus lung infection. Together, these data suggest that therapies targeting the gut microbiota are a promising approach to help treat post-acute COVID-19, although the effects of *B. longum* 5^{1A} must be explored further.

Our study sheds light on a possible direct connection between alterations in the microbiota and post-acute COVID-19 symptoms. Nevertheless, one of the main limitations of our study is the small sample size and the fact that we compared groups of individuals that were not perfectly age and sex-matched. In addition, other factors, such as the gut virome, could also play a role in host health and disease but were not analyzed here [102–106]. Indeed, alterations in the composition of the host virome have been reported to be associated with clinical outcomes of COVID-19 infection [107–109]. Finally, SARS-CoV-2 antigens can persist for long periods in the intestine, feces, and gut tissues of the patients, thus boosting immune responses that may fuel the symptoms of long-COVID [110, 111]. Nevertheless, we did not find any sign of SARS-CoV-2 in the feces of donor subjects and neither in the lung of humanized microbiota recipient mice. Despite these limitations, we believe our study is still very meaningful especially given the magnitude of what is still unknown about COVID-19.

Conclusion

Taken together, our results show direct causal effects of the gut microbiota from humans previously exposed to SARS-CoV2 in supporting the long-term effects of COVID-19 after infection clearance. Our findings also emphasize the need to study how the gut microbiota is affected by SARS-CoV-2 infection in subjects that did not manifest severe symptoms. This is especially concerning due to the increase in antimicrobial resistance in the gut microbiota of subjects previously infected with SARS-CoV2. Antimicrobial resistance is currently spreading at alarming rates and will certainly be accelerated by the COVID-19 pandemic mediated by the alterations induced in the gut microbiota resistome.

List Of Abbreviations

SARS-CoV-2
Severe acute respiratory syndrome coronavirus 2
COVID-19
Coronavirus disease 2019
HM
Humanized Microbiome

I-FABP
Intestinal fatty acid-binding protein
AMR
Antimicrobial resistance
TNF-α
Tumor necrosis factor-alpha
BDNF
Brain-derived neurotrophic factor
PSD-95
Postsynaptic density protein-95
ACE2
Angiotensin-converting enzyme 2
TMPRSS2
Type-II transmembrane serine proteases
LPS
Lipopolysaccharide
PSA
Polysaccharide A
FMT
Fecal microbiota transplant
GF
Germe-free
NAAT
Nucleic Acid Amplification Test
NHI
National Institutes of Health
CFU
Colony-forming unit
MHV-3
Mouse Hepatitis Virus strain-3
PFU
Plaque-forming unit
MRS
De Man, Rogosa, and Sharpe
BAL
Bronchoalveolar lavage
RT-qPCR
Real-Time quantitative PCR
CDC
Centers for Disease Control and Prevention

HPLC
High-Performance Liquid Chromatography
SCFAs
Short-chain fatty acids
H&E
Hematoxylin and eosin
MALDI-TOF
Matrix-Assisted Laser Desorption/Ionization-Time Of Flight
MDR
Multidrug resistance
KEGG
Kyoto Encyclopedia of Genes and Genomes
BBB
Blood-Brain Barrier

Declarations

Ethics approval and consent to participate

All participants consented to participate to this study under the Ethics Committee on Human Research of Universidade Federal de Minas Gerais (COEP) protocol 4.615.698. The animal study was reviewed and approved by The Institutional Committee for Animal Ethics of Universidade Federal de Minas Gerais (CEUA/UFMG–Licenses 281/2020 and 55/2021).

Consent for publication

Not applicable.

Availability of data and materials

The metagenomic libraries produced in this work were deposited in the NCBI SRA database under project number PRJNA843134

Competing interests

The authors declare that they have no competing interests to declare.

Funding

This work was supported by National Council for Scientific and Technological Development – CNPq (call MCTIC/CNPq/FNDCT/MS/SCTIE/Decit Nº 07/2020 - Universal MCTIC/CNPq 2018 and 2022). This study was financed in part by Coordenação de Aperfeiçoamento de Pessoal de Nível Superior, Brazil (CAPES) Finance Code 001. This study was supported by Fundação de Amparo à Pesquisa de Minas

Gerais (FAPEMIG) (APQ-03328-18; APQ-00686-21). This study was supported by Pró-Reitoria de Pesquisa da Universidade Federal de Minas Gerais - PRPq. This study was also supported by Instituto Serrapilheira (Nº 03/2019) and and São Paulo Research Foundation (grants 2017/25588-1, 2018/14666-4, 2019/00098-7, 2019/05155-9 and 2020/04746-0).

Authors' contributions

VM: conceptualization, methodology, investigation, formal analysis, data visualization, and original manuscript draft: review and editing. DFE: mouse behavioral tests, proteomics analysis, and original manuscript draft: review and editing. MFR: collected human samples, histopathology analysis, and manuscript original draft: review and editing. CSC: cultivable microbiota quantification, antimicrobial resistance tests and analysis, and data visualization. DAA: RT-qPCR quantification SARS-CoV2 and virome analysis. MA: SCFAs measurements. JM: clinical survey and curation data. ECM: cultivable microbiota quantification, antimicrobial resistance test. VMR: cultivable microbiota and bronchoalveolar lavage quantification. TGC: RT-qPCR quantification neurotrophic factor and analysis. LSBL and JCPG: MHV-3 experiments. IG: original manuscript draft: review and editing. MAS: mouse behavioral tests. ESR: survey methodology. GDC: histopathology analysis. RSS: I-FABP quantification and analysis. CCG: original manuscript draft: review and editing. MMT: provide MHV-3. VVC: MHV-3 facilities. LCA: SCFAs measurements. FSM: original manuscript draft: review and editing. FMR: RT-qPCR quantification neurotrophic factor and analysis. GSZ, BJS, VCC, and DMS: proteomic brain assays and analysis. ERGRA and ISL: microbiota 16S bioinformatics data analysis. JTM: conceptualization, investigation, RT-qPCR quantification SARS-CoV2, manuscript writing, review, and editing. ATV: conceptualization, investigation, formal analysis, supervision, resources, funding, project administration, manuscript writing, review, and editing. All authors reviewed the manuscript.

Acknowledgements

The authors thank the Laboratory of Gnotobiology coordinated by Prof Leda Quercia Vieira of the Department of Biochemistry and Immunology (UFMG) for the technical support with the GF mice facilities. Prof. Vasco Azevedo provided *K. pneumoniae* clinical isolate strain for the study. We also thank Daniela M. Nolasco for the technical support with SCFAs measurements in feces. The authors thank Eduardo Zimmer and Andreza F. de Bem for advice on cognitive experimental design and Ana Maria Caetano de Faria for valuable data discussions.

References

1. WHO. WHO Coronavirus (COVID-19) Dashboard [Internet]. 2022. Available from: WHO Coronavirus (COVID-19) Dashboard
2. Huang C, Huang L, Wang Y, Li X, Ren L, Gu X, et al. 6-month consequences of COVID-19 in patients discharged from hospital: a cohort study. Lancet (London, England) [Internet]. 2021;397:220–32. Available from: http://www.ncbi.nlm.nih.gov/pubmed/33428867

3. O'Sullivan O. Long-term sequelae following previous coronavirus epidemics. Clin Med [Internet]. 2021;21:e68–70. Available from: http://www.ncbi.nlm.nih.gov/pubmed/33144403
4. Dani M, Dirksen A, Taraborrelli P, Torocastro M, Panagopoulos D, Sutton R, et al. Autonomic dysfunction in "long COVID": rationale, physiology and management strategies. Clin Med [Internet]. 2021;21:e63–7. Available from: http://www.ncbi.nlm.nih.gov/pubmed/33243837
5. Mendelson M, Nel J, Blumberg L, Madhi SA, Dryden M, Stevens W, et al. Long-COVID: An evolving problem with an extensive impact. S Afr Med J [Internet]. 2020;111:10–2. Available from: http://www.ncbi.nlm.nih.gov/pubmed/33403997
6. Hikmet F, Méar L, Edvinsson Å, Micke P, Uhlén M, Lindskog C. The protein expression profile of ACE2 in human tissues. Mol Syst Biol [Internet]. 2020;16:e9610. Available from: http://www.ncbi.nlm.nih.gov/pubmed/32715618
7. Wang B, Zhang L, Wang Y, Dai T, Qin Z, Zhou F, et al. Alterations in microbiota of patients with COVID-19: potential mechanisms and therapeutic interventions. Signal Transduct Target Ther [Internet]. 2022;7:143. Available from: https://www.nature.com/articles/s41392-022-00986-0
8. Ou X, Liu Y, Lei X, Li P, Mi D, Ren L, et al. Characterization of spike glycoprotein of SARS-CoV-2 on virus entry and its immune cross-reactivity with SARS-CoV. Nat Commun [Internet]. 2020;11:1620. Available from: http://www.nature.com/articles/s41467-020-15562-9
9. Yeoh YK, Zuo T, Lui GC-Y, Zhang F, Liu Q, Li AY, et al. Gut microbiota composition reflects disease severity and dysfunctional immune responses in patients with COVID-19. Gut [Internet]. 2021;70:698–706. Available from: http://www.ncbi.nlm.nih.gov/pubmed/33431578
10. Levy M, Kolodziejczyk AA, Thaiss CA, Elinav E. Dysbiosis and the immune system. Nat. Rev. Immunol. Nature Publishing Group; 2017. p. 219–32.
11. Thursby E, Juge N. Introduction to the human gut microbiota. Biochem. J. Portland Press Ltd; 2017. p. 1823–36.
12. Sencio V, Gallerand A, Gomes Machado M, Deruyter L, Heumel S, Soulard D, et al. Influenza Virus Infection Impairs the Gut's Barrier Properties and Favors Secondary Enteric Bacterial Infection through Reduced Production of Short-Chain Fatty Acids. Infect Immun [Internet]. 2021;89:e0073420. Available from: http://www.ncbi.nlm.nih.gov/pubmed/33820816
13. Sencio V, Barthelemy A, Tavares LP, Machado MG, Soulard D, Cuinat C, et al. Gut Dysbiosis during Influenza Contributes to Pulmonary Pneumococcal Superinfection through Altered Short-Chain Fatty Acid Production. Cell Rep [Internet]. 2020;30:2934–2947.e6. Available from: http://www.ncbi.nlm.nih.gov/pubmed/32130898
14. Gu S, Chen Y, Wu Z, Chen Y, Gao H, Lv L, et al. Alterations of the Gut Microbiota in Patients With Coronavirus Disease 2019 or H1N1 Influenza. Clin Infect Dis [Internet]. 2020;71:2669–78. Available from: https://academic.oup.com/cid/article/71/10/2669/5851452
15. de Oliveira GLV, Oliveira CNS, Pinzan CF, de Salis LVV, Cardoso CR de B. Microbiota Modulation of the Gut-Lung Axis in COVID-19. Front Immunol [Internet]. 2021;12. Available from: https://www.frontiersin.org/articles/10.3389/fimmu.2021.635471/full

16. Zuo T, Zhang F, Lui GCY, Yeoh YK, Li AYL, Zhan H, et al. Alterations in Gut Microbiota of Patients With COVID-19 During Time of Hospitalization. Gastroenterology. Elsevier, Inc; 2020;159:944–955.e8.
17. Chen Y, Gu S, Chen Y, Lu H, Shi D, Guo J, et al. Six-month follow-up of gut microbiota richness in patients with COVID-19. Gut [Internet]. 2022;71:222–5. Available from: https://gut.bmj.com/lookup/doi/10.1136/gutjnl-2021-324090
18. Zuo T, Liu Q, Zhang F, Lui GCY, Tso EYK, Yeoh YK, et al. Depicting SARS-CoV-2 faecal viral activity in association with gut microbiota composition in patients with COVID-19. Gut. 2021;70:276–84.
19. Liu Q, Mak JWY, Su Q, Yeoh YK, Lui GC-Y, Ng SSS, et al. Gut microbiota dynamics in a prospective cohort of patients with post-acute COVID-19 syndrome. Gut [Internet]. 2022;71:544–52. Available from: https://gut.bmj.com/lookup/doi/10.1136/gutjnl-2021-325989
20. Dang AT, Marsland BJ. Microbes, metabolites, and the gut–lung axis. Mucosal Immunol [Internet]. 2019;12:843–50. Available from: http://www.nature.com/articles/s41385-019-0160-6
21. Cullen BR. MicroRNAs as mediators of viral evasion of the immune system. Nat Immunol [Internet]. 2013;14:205–10. Available from: http://www.ncbi.nlm.nih.gov/pubmed/23416678
22. Aydemir MN, Aydemir HB, Korkmaz EM, Budak M, Cekin N, Pinarbasi E. Computationally predicted SARS-COV-2 encoded microRNAs target NFKB, JAK/STAT and TGFB signaling pathways. Gene reports [Internet]. 2021;22:101012. Available from: http://www.ncbi.nlm.nih.gov/pubmed/33398248
23. Lehnardt S, Lachance C, Patrizi S, Lefebvre S, Follett PL, Jensen FE, et al. The Toll-Like Receptor TLR4 Is Necessary for Lipopolysaccharide-Induced Oligodendrocyte Injury in the CNS. J Neurosci [Internet]. 2002;22:2478–86. Available from: https://www.jneurosci.org/lookup/doi/10.1523/JNEUROSCI.22-07-02478.2002
24. Maslowski KM, Vieira AT, Ng A, Kranich J, Sierro F, Yu D, et al. Regulation of inflammatory responses by gut microbiota and chemoattractant receptor GPR43. Nature. 2009;461:1282–6.
25. Fagundes CT, Amaral FA, Vieira AT, Soares AC, Pinho V, Nicoli JR, et al. Transient TLR Activation Restores Inflammatory Response and Ability To Control Pulmonary Bacterial Infection in Germfree Mice. J Immunol. 2012;188:1411–20.
26. Isles NS, Mu A, Kwong JC, Howden BP, Stinear TP. Gut microbiome signatures and host colonization with multidrug-resistant bacteria. Trends Microbiol. 2022;
27. Xu L, Surathu A, Raplee I, Chockalingam A, Stewart S, Walker L, et al. The effect of antibiotics on the gut microbiome: a metagenomics analysis of microbial shift and gut antibiotic resistance in antibiotic treated mice. BMC Genomics. 2020;21:263.
28. Kariyawasam RM, Julien DA, Jelinski DC, Larose SL, Rennert-May E, Conly JM, et al. Antimicrobial resistance (AMR) in COVID-19 patients: a systematic review and meta-analysis (November 2019–June 2021). Antimicrob Resist Infect Control. 2022;11:45.
29. Afshinnekoo E, Bhattacharya C, Burguete-García A, Castro-Nallar E, Deng Y, Desnues C, et al. COVID-19 drug practices risk antimicrobial resistance evolution. The Lancet Microbe. 2021;2:e135–6.
30. Karataş M, Yaşar-Duman M, Tünger A, Çilli F, Aydemir Ş, Özenci V. Secondary bacterial infections and antimicrobial resistance in COVID-19: comparative evaluation of pre-pandemic and pandemic-era, a

retrospective single center study. Ann Clin Microbiol Antimicrob. 2021;20:51.

31. Martinez-Guerra BA, Gonzalez-Lara MF, De-Leon-Cividanes NA, Tamez-Torres KM, Roman-Montes CM, Rajme-Lopez S, et al. Antimicrobial Resistance Patterns and Antibiotic Use during Hospital Conversion in the COVID-19 Pandemic. Antibiotics. 2021;10:182.
32. Pamer EG. Resurrecting the intestinal microbiota to combat antibiotic-resistant pathogens. Science [Internet]. 2016;352:535–8. Available from: http://www.ncbi.nlm.nih.gov/pubmed/27126035
33. Wischmeyer PE, Tang H, Ren Y, Bohannon L, Ramirez ZE, Andermann TM, et al. Daily Lactobacillus Probiotic versus Placebo in COVID-19-Exposed Household Contacts (PROTECT-EHC): A Randomized Clinical Trial. medRxiv. Cold Spring Harbor Laboratory Press; 2022;
34. National Institutes of Health. Coronavirus Disease 2019 (COVID-19) Treatment Guidelines [Internet]. 2022. Available from: https://www.covid19treatmentguidelines.nih.gov/
35. Pleasants JR. Gnotobiotics. Melby ECJ, Altman NH, editors. Cleveland: CRC Press; 1974.
36. Vieira AT, Macia L, Galvão I, Martins FS, Canesso MCC, Amaral FA, et al. A role for gut microbiota and the metabolite-sensing receptor GPR43 in a murine model of gout. Arthritis Rheumatol. John Wiley and Sons Inc.; 2015;67:1646–56.
37. Profeta R, Seyffert N, Tiwari S, Viana MVC, Jaiswal AK, Caetano AC, et al. Comparative genomics with a multidrug-resistant Klebsiella pneumoniae isolate reveals the panorama of unexplored diversity in Northeast Brazil. Gene [Internet]. 2021;772:145386. Available from: https://linkinghub.elsevier.com/retrieve/pii/S0378111920310556
38. Vieira AT, Rocha VM, Tavares L, Garcia CC, Teixeira MM, Oliveira SC, et al. Control of Klebsiella pneumoniae pulmonary infection and immunomodulation by oral treatment with the commensal probiotic Bifidobacterium longum 5(1A). Microbes Infect [Internet]. 2016;18:180–9. Available from: http://www.ncbi.nlm.nih.gov/pubmed/26548605
39. Andrade AC dos SP, Campolina-Silva GH, Queiroz-Junior CM, de Oliveira LC, Lacerda L de SB, Gaggino JCP, et al. A Biosafety Level 2 Mouse Model for Studying Betacoronavirus-Induced Acute Lung Damage and Systemic Manifestations. Schultz-Cherry S, editor. J Virol [Internet]. 2021;95. Available from: https://journals.asm.org/doi/10.1128/JVI.01276-21
40. da Silva JGV, Vieira AT, Sousa TJ, Viana MVC, Parise D, Sampaio B, et al. Comparative genomics and in silico gene evaluation involved in the probiotic potential of Bifidobacterium longum 51A. Gene [Internet]. 2021;795:145781. Available from: https://linkinghub.elsevier.com/retrieve/pii/S0378111921003760
41. Melo HM, Seixas da Silva G da S, Sant'Ana MR, Teixeira CVL, Clarke JR, Miya Coreixas VS, et al. Palmitate Is Increased in the Cerebrospinal Fluid of Humans with Obesity and Induces Memory Impairment in Mice via Pro-inflammatory TNF-α. Cell Rep [Internet]. 2020;30:2180–2194.e8. Available from: https://linkinghub.elsevier.com/retrieve/pii/S2211124720300978
42. Coryell MP, Iakiviak M, Pereira N, Murugkar PP, Rippe J, Williams DB, et al. A method for detection of SARS-CoV-2 RNA in healthy human stool: a validation study. The Lancet Microbe [Internet]. 2021;2:e259–66. Available from: https://linkinghub.elsevier.com/retrieve/pii/S2666524721000598

43. Prevention C for DC and. CDC 2019-novel coronavirus (2019-nCoV) real-time RT-PCR diagnostic panel. 2020;
44. Saia RS, Giusti H, Luis-Silva F, Pedroso K de JB, Auxiliadora-Martins M, Morejón KML, et al. Clinical investigation of intestinal fatty acid-binding protein (I-FABP) as a biomarker of SARS-CoV-2 infection. Int J Infect Dis [Internet]. 2021;113:82–6. Available from: https://linkinghub.elsevier.com/retrieve/pii/S120197122100761X
45. Gallotti B, Galvao I, Leles G, Quintanilha MF, Souza RO, Miranda VC, et al. Effects of dietary fibre intake in chemotherapy-induced mucositis in murine model. Br J Nutr [Internet]. 2020;1–12. Available from: https://www.cambridge.org/core/product/identifier/S0007114520004924/type/journal_article
46. Wang C, Chen Y, Tain Y, Chang SKC, Huang L, Hsieh C, et al. Fast quantification of short-chain fatty acids in rat plasma by gas chromatography. J Food Sci. Wiley Online Library; 2020;85:1932–8.
47. Horvat JC, Beagley KW, Wade MA, Preston JA, Hansbro NG, Hickey DK, et al. Neonatal Chlamydial Infection Induces Mixed T-Cell Responses That Drive Allergic Airway Disease. Am J Respir Crit Care Med [Internet]. 2007;176:556–64. Available from: http://www.atsjournals.org/doi/abs/10.1164/rccm.200607-1005OC
48. Garcia CC, Russo RC, Guabiraba R, Fagundes CT, Polidoro RB, Tavares LP, et al. Platelet-Activating Factor Receptor Plays a Role in Lung Injury and Death Caused by Influenza A in Mice. Fouchier RAM, editor. PLoS Pathog [Internet]. 2010;6:e1001171. Available from: https://dx.plos.org/10.1371/journal.ppat.1001171
49. Nakagaki KY, Nunes MM, Garcia AP V, Nunes FC, Schmitt F, Cassali GD. Solid Carcinoma of the Canine Mammary Gland: a Histological Type or Tumour Cell Arrangement? J Comp Pathol [Internet]. 2022;190:1–12. Available from: https://linkinghub.elsevier.com/retrieve/pii/S0021997521001389
50. Assis GBN, Pereira FL, Zegarra AU, Tavares GC, Leal CA, Figueiredo HCP. Use of MALDI-TOF Mass Spectrometry for the Fast Identification of Gram-Positive Fish Pathogens. Front Microbiol [Internet]. 2017;8. Available from: http://journal.frontiersin.org/article/10.3389/fmicb.2017.01492/full
51. Bastian M, Heymann S, Jacomy M. Gephi: An Open Source Software for Exploring and Manipulating Networks [Internet]. 2009. p. 2. Available from: https://ojs.aaai.org/index.php/ICWSM/article/view/13937
52. Distler U, Kuharev J, Navarro P, Tenzer S. Label-free quantification in ion mobility–enhanced data-independent acquisition proteomics. Nat Protoc [Internet]. 2016;11:795–812. Available from: http://www.nature.com/articles/nprot.2016.042
53. Huang DW, Sherman BT, Lempicki RA. Systematic and integrative analysis of large gene lists using DAVID bioinformatics resources. Nat Protoc [Internet]. 2009;4:44–57. Available from: http://www.nature.com/articles/nprot.2008.211
54. Amplicon PCR, Clean-Up PCR, Index PCR. 16s metagenomic sequencing library preparation. Illumina San Diego, CA, USA. 2013;
55. Bolyen E, Rideout JR, Dillon MR, Bokulich NA, Abnet CC, Al-Ghalith GA, et al. Reproducible, interactive, scalable and extensible microbiome data science using QIIME 2. Nat Biotechnol [Internet].

2019;37:852–7. Available from: http://www.nature.com/articles/s41587-019-0209-9

56. Rognes T, Flouri T, Nichols B, Quince C, Mahé F. VSEARCH: a versatile open source tool for metagenomics. PeerJ [Internet]. 2016;4:e2584. Available from: https://peerj.com/articles/2584
57. Quast C, Pruesse E, Yilmaz P, Gerken J, Schweer T, Yarza P, et al. The SILVA ribosomal RNA gene database project: improved data processing and web-based tools. Nucleic Acids Res [Internet]. 2012;41:D590–6. Available from: http://academic.oup.com/nar/article/41/D1/D590/1069277/The-SILVA-ribosomal-RNA-gene-database-project
58. Caugant DA, Levin BR, Selander RK. Distribution of multilocus genotypes of Escherichia coli within and between host families. J Hyg (Lond) [Internet]. 1984;92:377–84. Available from: https://www.cambridge.org/core/product/identifier/S0022172400064597/type/journal_article
59. Song SJ, Lauber C, Costello EK, Lozupone CA, Humphrey G, Berg-Lyons D, et al. Cohabiting family members share microbiota with one another and with their dogs. Elife [Internet]. 2013;2. Available from: https://elifesciences.org/articles/00458
60. Schloss PD, Iverson KD, Petrosino JF, Schloss SJ. The dynamics of a family's gut microbiota reveal variations on a theme. Microbiome [Internet]. 2014;2:25. Available from: https://microbiomejournal.biomedcentral.com/articles/10.1186/2049-2618-2-25
61. Livanos AE, Jha D, Cossarini F, Gonzalez-Reiche AS, Tokuyama M, Aydillo T, et al. Intestinal Host Response to SARS-CoV-2 Infection and COVID-19 Outcomes in Patients With Gastrointestinal Symptoms. Gastroenterology. 2021;160:2435–2450.e34.
62. Wu Y, Cheng X, Jiang G, Tang H, Ming S, Tang L, et al. Altered oral and gut microbiota and its association with SARS-CoV-2 viral load in COVID-19 patients during hospitalization. npj Biofilms Microbiomes. 2021;7:61.
63. Van Laethem J, Wuyts S, Van Laere S, Koulalis J, Colman M, Moretti M, et al. Antibiotic prescriptions in the context of suspected bacterial respiratory tract superinfections in the COVID-19 era: a retrospective quantitative analysis of antibiotic consumption and identification of antibiotic prescription drivers. Intern Emerg Med. 2022;17:141–51.
64. Karami Z, Knoop BT, Dofferhoff ASM, Blaauw MJT, Janssen NA, van Apeldoorn M, et al. Few bacterial co-infections but frequent empiric antibiotic use in the early phase of hospitalized patients with COVID-19: results from a multicentre retrospective cohort study in The Netherlands. Infect Dis (Auckl). 2021;53:102–10.
65. Hinks TSC, Cureton L, Knight R, Wang A, Cane JL, Barber VS, et al. Azithromycin versus standard care in patients with mild-to-moderate COVID-19 (ATOMIC2): an open-label, randomised trial. Lancet Respir Med. 2021;9:1130–40.
66. Tsay S V., Bartoces M, Gouin K, Kabbani S, Hicks LA. Antibiotic Prescriptions Associated With COVID-19 Outpatient Visits Among Medicare Beneficiaries, April 2020 to April 2021. JAMA. 2022;
67. Oldenburg CE, Pinsky BA, Brogdon J, Chen C, Ruder K, Zhong L, et al. Effect of Oral Azithromycin vs Placebo on COVID-19 Symptoms in Outpatients With SARS-CoV-2 Infection. JAMA. 2021;326:490.

68. Kamel AM, Monem MSA, Sharaf NA, Magdy N, Farid SF. Efficacy and safety of azithromycin in Covid-19 patients: A systematic review and meta-analysis of randomized clinical trials. Rev Med Virol. 2022;32.
69. Cavalcanti AB, Zampieri FG, Rosa RG, Azevedo LCP, Veiga VC, Avezum A, et al. Hydroxychloroquine with or without Azithromycin in Mild-to-Moderate Covid-19. N Engl J Med. 2020;383:2041–52.
70. Furlan L, Caramelli B. The regrettable story of the “Covid Kit” and the “Early Treatment of Covid-19” in Brazil. Lancet Reg Heal - Am. 2021;4:100089.
71. Bahçe YG, Acer Ö, Özüdoğru O. Evaluation of bacterial agents isolated from endotracheal aspirate cultures of Covid-19 general intensive care patients and their antibiotic resistance profiles compared to pre-pandemic conditions. Microb Pathog. 2022;164:105409.
72. Bazaid AS, Barnawi H, Qanash H, Alsaif G, Aldarhami A, Gattan H, et al. Bacterial Coinfection and Antibiotic Resistance Profiles among Hospitalised COVID-19 Patients. Microorganisms. 2022;10:495.
73. Langford BJ, So M, Raybardhan S, Leung V, Westwood D, MacFadden DR, et al. Bacterial co-infection and secondary infection in patients with COVID-19: a living rapid review and meta-analysis. Clin Microbiol Infect. 2020;26.
74. Shafran N, Shafran I, Ben-Zvi H, Sofer S, Sheena L, Krause I, et al. Secondary bacterial infection in COVID-19 patients is a stronger predictor for death compared to influenza patients. Sci Rep. 2021;11.
75. Budden KF, Gellatly SL, Wood DLA, Cooper MA, Morrison M, Hugenholtz P, et al. Emerging pathogenic links between microbiota and the gut–lung axis. Nat Rev Microbiol. 2017;15:55–63.
76. Jang YO, Kim OH, Kim SJ, Lee SH, Yun S, Lim SE, et al. High-fiber diets attenuate emphysema development via modulation of gut microbiota and metabolism. Sci Rep. Nature Research; 2021;11:1–11.
77. Govers C, Tomassen MMM, Rieder A, Ballance S, Knutsen SH, Mes JJ. Lipopolysaccharide quantification and alkali-based inactivation in polysaccharide preparations to enable in vitro immune modulatory studies. Bioact Carbohydrates Diet Fibre. 2016;8:15–25.
78. Huffnagle GB, Dickson RP, Lukacs NW. The respiratory tract microbiome and lung inflammation: a two-way street. Mucosal Immunol. 2017;10:299–306.
79. Morais LH, Schreiber HL, Mazmanian SK. The gut microbiota-brain axis in behaviour and brain disorders. Nat Rev Microbiol. 2021;19:241–55.
80. Cryan JF, O’riordan KJ, Cowan CSM, Sandhu K V., Bastiaanssen TFS, Boehme M, et al. The microbiota-gut-brain axis. Physiol Rev. American Physiological Society; 2019;99:1877–2013.
81. Bajinka O, Simbilyabo L, Tan Y, Jabang J, Saleem SA. Lung-brain axis. Crit Rev Microbiol. 2022;48:257–69.
82. Hosang L, Canals RC, van der Flier FJ, Hollensteiner J, Daniel R, Flügel A, et al. The lung microbiome regulates brain autoimmunity. Nature. 2022;603:138–44.
83. Yang I, Arthur RA, Zhao L, Clark J, Hu Y, Corwin EJ, et al. The oral microbiome and inflammation in mild cognitive impairment. Exp Gerontol. 2021;147:111273.

84. Liu X-X, Jiao B, Liao X-X, Guo L-N, Yuan Z-H, Wang X, et al. Analysis of Salivary Microbiome in Patients with Alzheimer's Disease. J Alzheimers Dis. 2019;72:633–40.
85. Erny D, Hrabě de Angelis AL, Jaitin D, Wieghofer P, Staszewski O, David E, et al. Host microbiota constantly control maturation and function of microglia in the CNS. Nat Neurosci [Internet]. 2015;18:965–77. Available from: http://www.nature.com/articles/nn.4030
86. Al-Aly Z, Xie Y, Bowe B. High-dimensional characterization of post-acute sequelae of COVID-19. Nature. 2021;594:259–64.
87. Taquet M, Geddes JR, Husain M, Luciano S, Harrison PJ. 6-month neurological and psychiatric outcomes in 236 379 survivors of COVID-19: a retrospective cohort study using electronic health records. The lancet Psychiatry. 2021;8:416–27.
88. Bowerman KL, Rehman SF, Vaughan A, Lachner N, Budden KF, Kim RY, et al. Disease-associated gut microbiome and metabolome changes in patients with chronic obstructive pulmonary disease. Nat Commun. Nature Research; 2020;11:1–15.
89. Zhang L, Wang Y, Xiayu X, Shi C, Chen W, Song N, et al. Altered Gut Microbiota in a Mouse Model of Alzheimer's Disease. J Alzheimer's Dis [Internet]. 2017;60:1241–57. Available from: https://www.medra.org/servlet/aliasResolver?alias=iospress&doi=10.3233/JAD-170020
90. Doifode T, Giridharan V V., Generoso JS, Bhatti G, Collodel A, Schulz PE, et al. The impact of the microbiota-gut-brain axis on Alzheimer's disease pathophysiology. Pharmacol Res [Internet]. 2021;164:105314. Available from: https://linkinghub.elsevier.com/retrieve/pii/S1043661820316224
91. Ho L, Ono K, Tsuji M, Mazzola P, Singh R, Pasinetti GM. Protective roles of intestinal microbiota derived short chain fatty acids in Alzheimer's disease-type beta-amyloid neuropathological mechanisms. Expert Rev Neurother [Internet]. 2018;18:83–90. Available from: https://www.tandfonline.com/doi/full/10.1080/14737175.2018.1400909
92. Falomir-Lockhart LJ, Cavazzutti GF, Giménez E, Toscani AM. Fatty Acid Signaling Mechanisms in Neural Cells: Fatty Acid Receptors. Front Cell Neurosci [Internet]. 2019;13. Available from: https://www.frontiersin.org/article/10.3389/fncel.2019.00162/full
93. Park J, Wang Q, Wu Q, Mao-Draayer Y, Kim CH. Bidirectional regulatory potentials of short-chain fatty acids and their G-protein-coupled receptors in autoimmune neuroinflammation. Sci Rep [Internet]. 2019;9:8837. Available from: http://www.nature.com/articles/s41598-019-45311-y
94. Sampson TR, Mazmanian SK. Control of brain development, function, and behavior by the microbiome. Cell Host Microbe. Cell Press; 2015. p. 565–76.
95. Jang S-E, Lim S-M, Jeong J-J, Jang H-M, Lee H-J, Han MJ, et al. Gastrointestinal inflammation by gut microbiota disturbance induces memory impairment in mice. Mucosal Immunol. 2018;11:369–79.
96. Jang H-M, Lee H-J, Jang S-E, Han MJ, Kim D-H. Evidence for interplay among antibacterial-induced gut microbiota disturbance, neuro-inflammation, and anxiety in mice. Mucosal Immunol. 2018;11:1386–97.
97. Kim N, Jeon SH, Ju IG, Gee MS, Do J, Oh MS, et al. Transplantation of gut microbiota derived from Alzheimer's disease mouse model impairs memory function and neurogenesis in C57BL/6 mice.

Brain Behav Immun. 2021;98:357–65.

98. Diaz Heijtz R, Wang S, Anuar F, Qian Y, Björkholm B, Samuelsson A, et al. Normal gut microbiota modulates brain development and behavior. Proc Natl Acad Sci U S A. 2011;108:3047–52.
99. Vieira AT, Galvão I, Amaral FA, Teixeira MM, Nicoli JR, Martins FS. Oral treatment with Bifidobacterium longum 51A reduced inflammation in a murine experimental model of gout. Benef Microbes [Internet]. 2015;6:799–806. Available from: http://www.ncbi.nlm.nih.gov/pubmed/26322542
100. He S, Wang L, Miao L, Wang T, Du F, Zhao L, et al. Receptor interacting protein kinase-3 determines cellular necrotic response to TNF-alpha. Cell. 2009;137:1100–11.
101. Jayaraman A, Htike TT, James R, Picon C, Reynolds R. TNF-mediated neuroinflammation is linked to neuronal necroptosis in Alzheimer's disease hippocampus. Acta Neuropathol Commun. 2021;9:159.
102. Breitbart M, Haynes M, Kelley S, Angly F, Edwards RA, Felts B, et al. Viral diversity and dynamics in an infant gut. Res Microbiol [Internet]. 2008;159:367–73. Available from: https://linkinghub.elsevier.com/retrieve/pii/S0923250808000648
103. Haynes M, Rohwer F. The Human Virome. Metagenomics Hum Body [Internet]. New York, NY: Springer New York; 2011. p. 63–77. Available from: http://link.springer.com/10.1007/978-1-4419-7089-3_4
104. Virgin HW, Wherry EJ, Ahmed R. Redefining Chronic Viral Infection. Cell [Internet]. 2009;138:30–50. Available from: https://linkinghub.elsevier.com/retrieve/pii/S0092867409007831
105. Yuan L, Hensley C, Mahsoub HM, Ramesh AK, Zhou P. Microbiota in viral infection and disease in humans and farm animals. 2020. p. 15–60. Available from: https://linkinghub.elsevier.com/retrieve/pii/S1877117320300491
106. Mukhopadhya I, Segal JP, Carding SR, Hart AL, Hold GL. The gut virome: the "missing link" between gut bacteria and host immunity? Therap Adv Gastroenterol. 2019;12:1756284819836620.
107. Zuo T, Liu Q, Zhang F, Yeoh YK, Wan Y, Zhan H, et al. Temporal landscape of human gut RNA and DNA virome in SARS-CoV-2 infection and severity. Microbiome. BioMed Central; 2021;9:91.
108. Lu Z-H, Zhou H-W, Wu W-K, Fu T, Yan M, He Z, et al. Alterations in the Composition of Intestinal DNA Virome in Patients With COVID-19. Front. Cell. Infect. Microbiol.. 2021.
109. Cao J, Wang C, Zhang Y, Lei G, Xu K, Zhao N, et al. Integrated gut virome and bacteriome dynamics in COVID-19 patients. Gut Microbes. 2021;13:1–21.
110. Natarajan A, Zlitni S, Brooks EF, Vance SE, Dahlen A, Hedlin H, et al. Gastrointestinal symptoms and fecal shedding of SARS-CoV-2 RNA suggest prolonged gastrointestinal infection. Med. 2022;
111. Zollner A, Koch R, Jukic A, Pfister A, Meyer M, Rössler A, et al. Post-acute COVID-19 is characterized by gut viral antigen persistence in inflammatory bowel diseases. Gastroenterology. 2022;

Figures

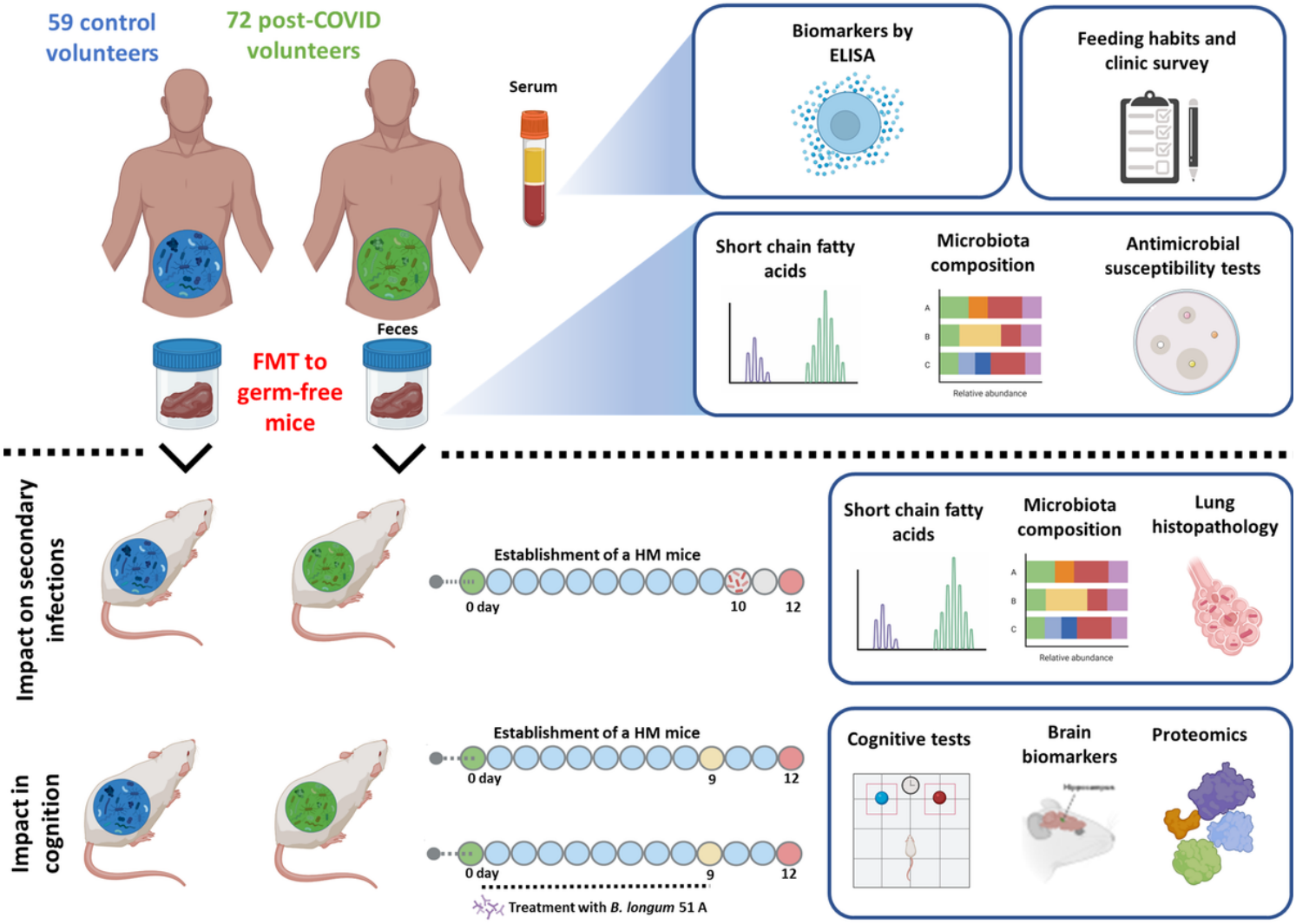

Figure 1

Schematic diagram illustrating the study design and procedure used in the study. Graphical study design was created with biorender.com (accessed on 05 May 2022).

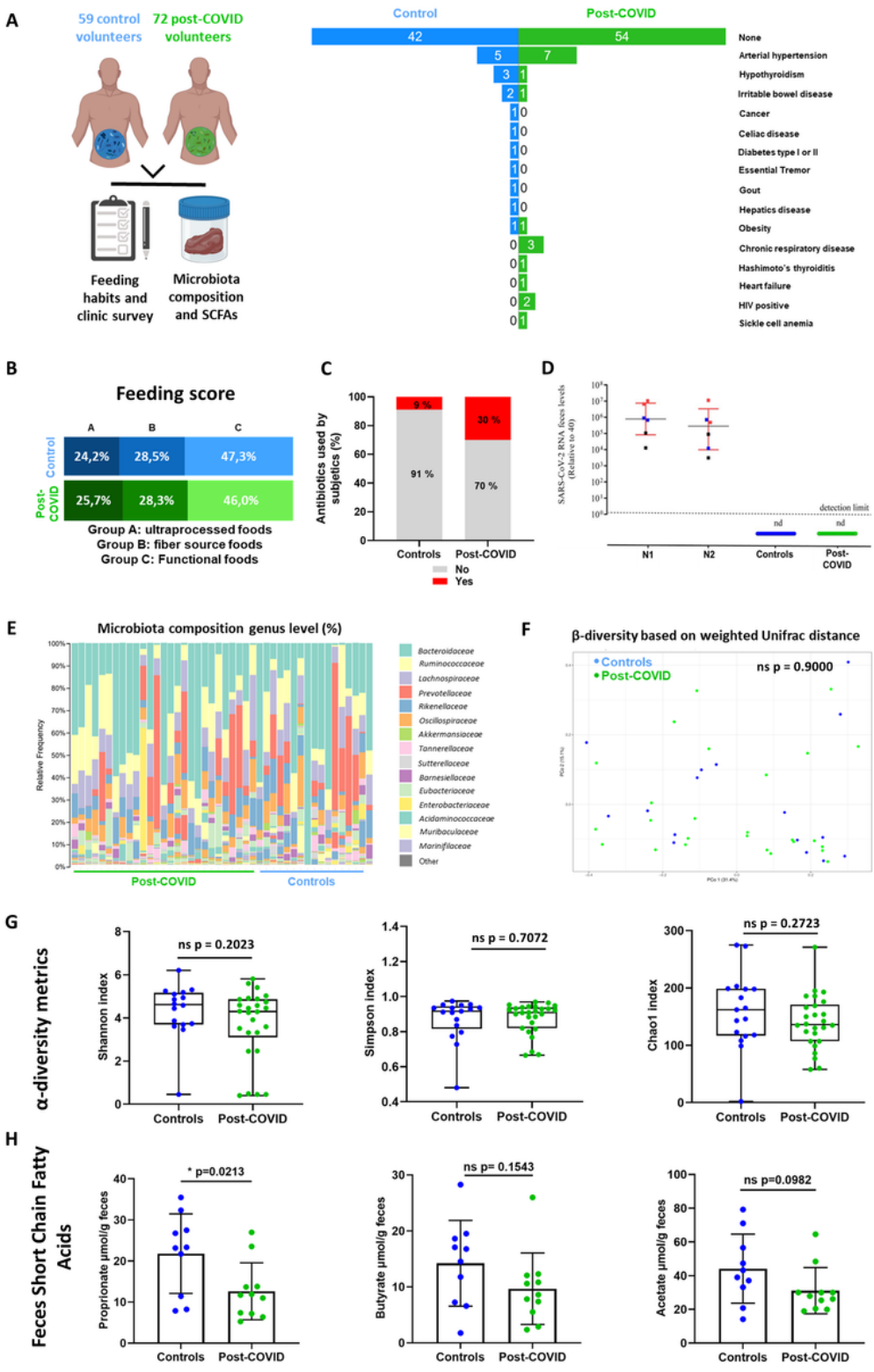

Figure 2

Association of clinical characteristics, food habits with the intestinal microbiota composition of controls and post-COVID human subjects. **A** Graphical representation of the study design and types of comorbidities in controls and post-COVID groups. **B** Feeding score according to Brazilian food. **C** Controls and post-COVID treated with antibiotics. **D** Quantification of SARS-CoV-2 by RT-qPCR in the feces of control and post-COVID. **E** 16S metagenomic analysis of gut microbiota composition from controls and

post-COVID subjects at the family level. **F** Principal Component Analysis based on weighted Unifrac distances (p = 0.9)**. G** Shannon, Simpson, and Chao1 indexes for α- diversity metrics**. H** Propionate, butyrate, and acetate concentrations (µmol/g) of post-COVID compared to controls. Statistical analysis: PerMANOVA pairwise test and Student's *t*-test. Data are shown as mean and standard deviation (SD).

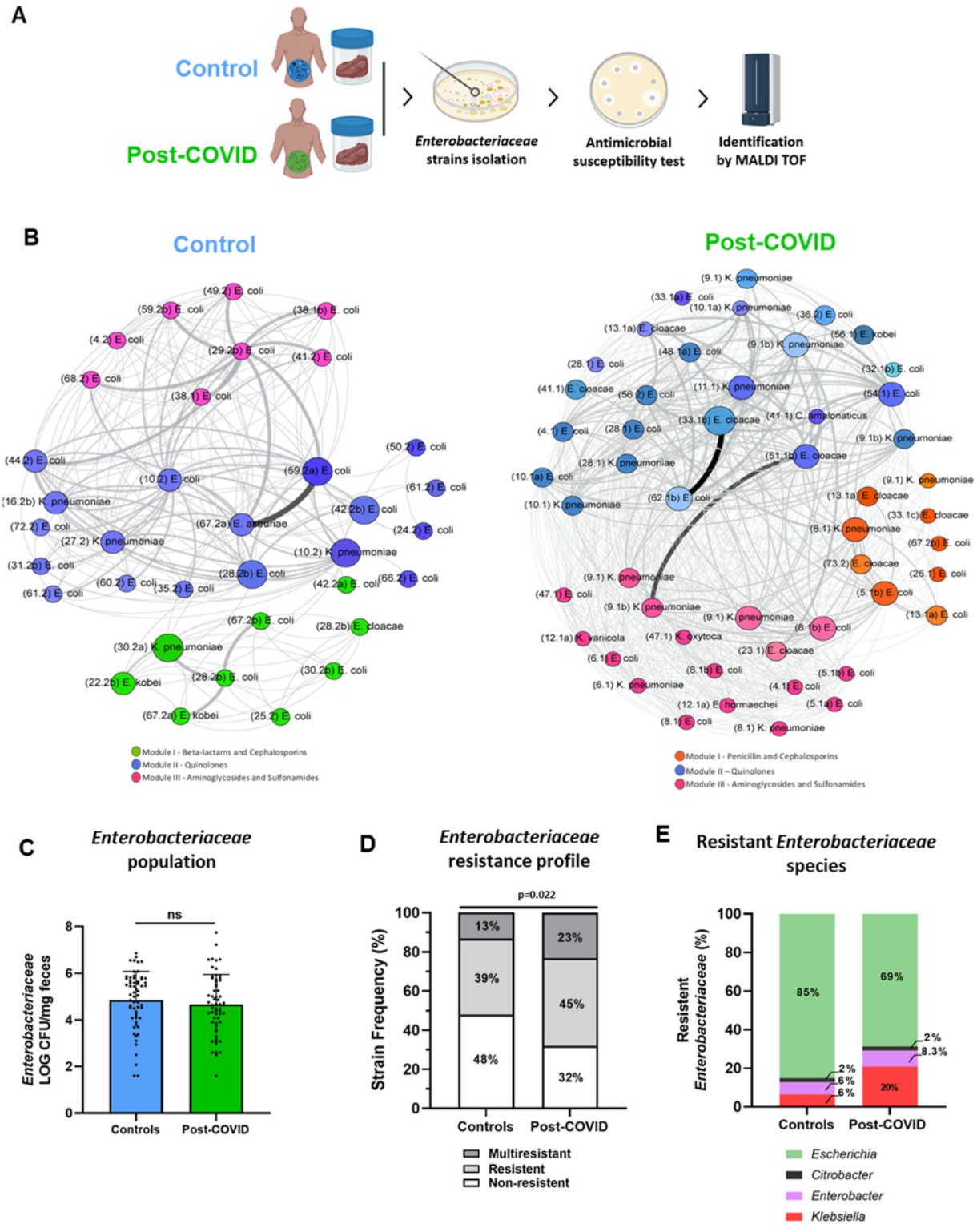

Figure 3

Resistance profile in *Enterobacteriaceae* species of controls and post-COVID human subjects. **A** Graphical representation of the study design. **B** Associations of bacteria species in antimicrobial susceptibility profile to *Enterobacteriaceae* isolates. **C** Quantification of *Enterobacteriaceae* population. **D** Percentage of *Enterobacteriaceae* strain frequency as a phenotype of multiresistant, resistance, and non-resistance profiles. **E** Percentage of resistant *Enterobacteriaceae* species. Statistical analysis: Student's *t*-test and Chi-square test. Data are shown as mean and standard deviation (SD).

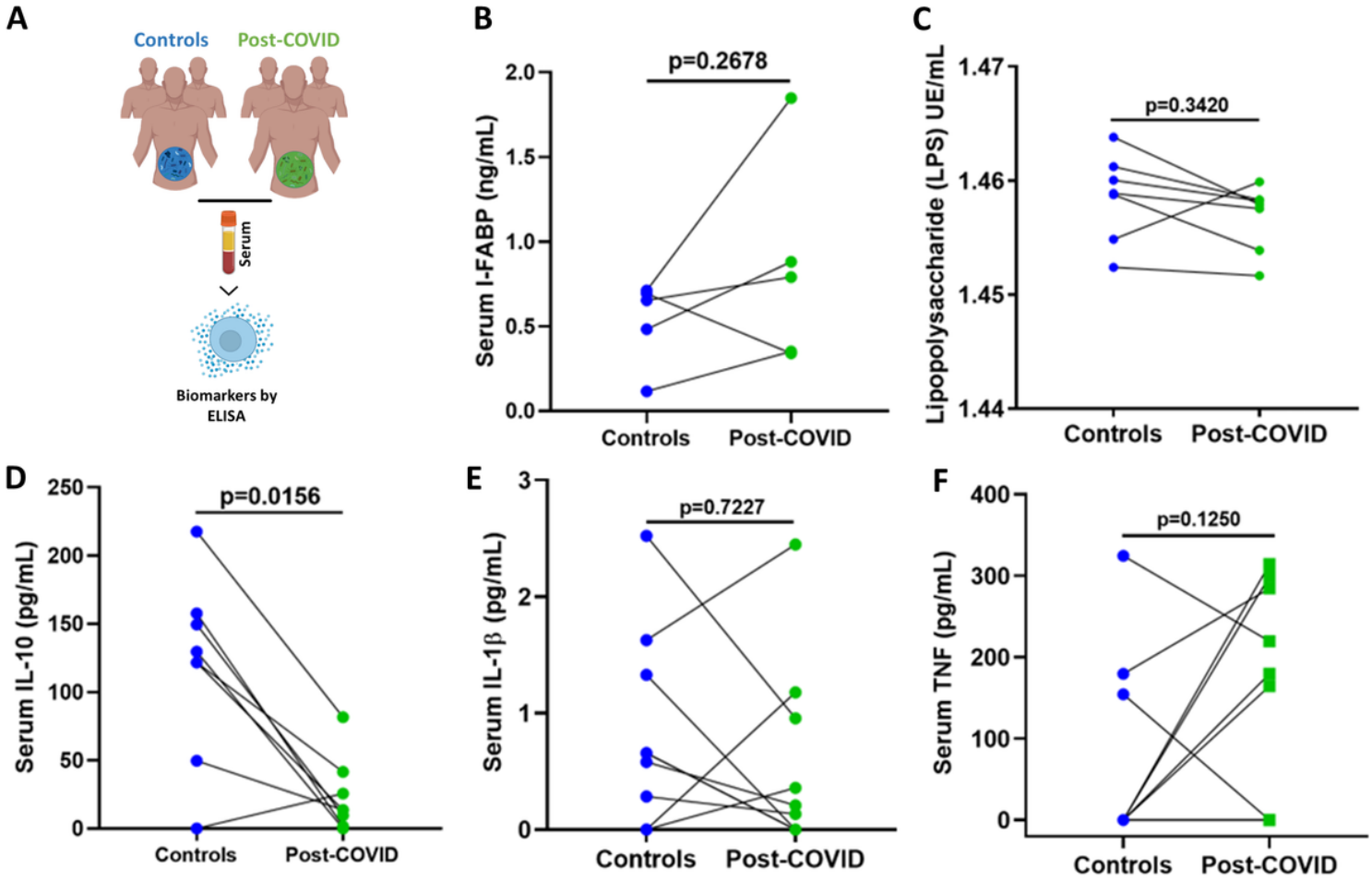

Figure 4

Correlated intestinal barrier injury and profile of cytokines of controls and post-COVID human subjects. Samples of serum were obtained from the human participant's controls and post-COVID (2 – 4 months post-diagnosis for SARS-CoV-2). **A** Graphical representation of the study design. **B** Quantification of lipopolysaccharide (UE/mL); **C** I-FABP (ng/mL); **D** IL-10; **E** IL-1β and **F** TNFa (pg/mL); of post-COVID compared to controls. Statistical analysis: Paired Student's *t*-test. Data are shown as mean and standard deviation (SD). Number of families (N = 11). Each data point represents the FMT.

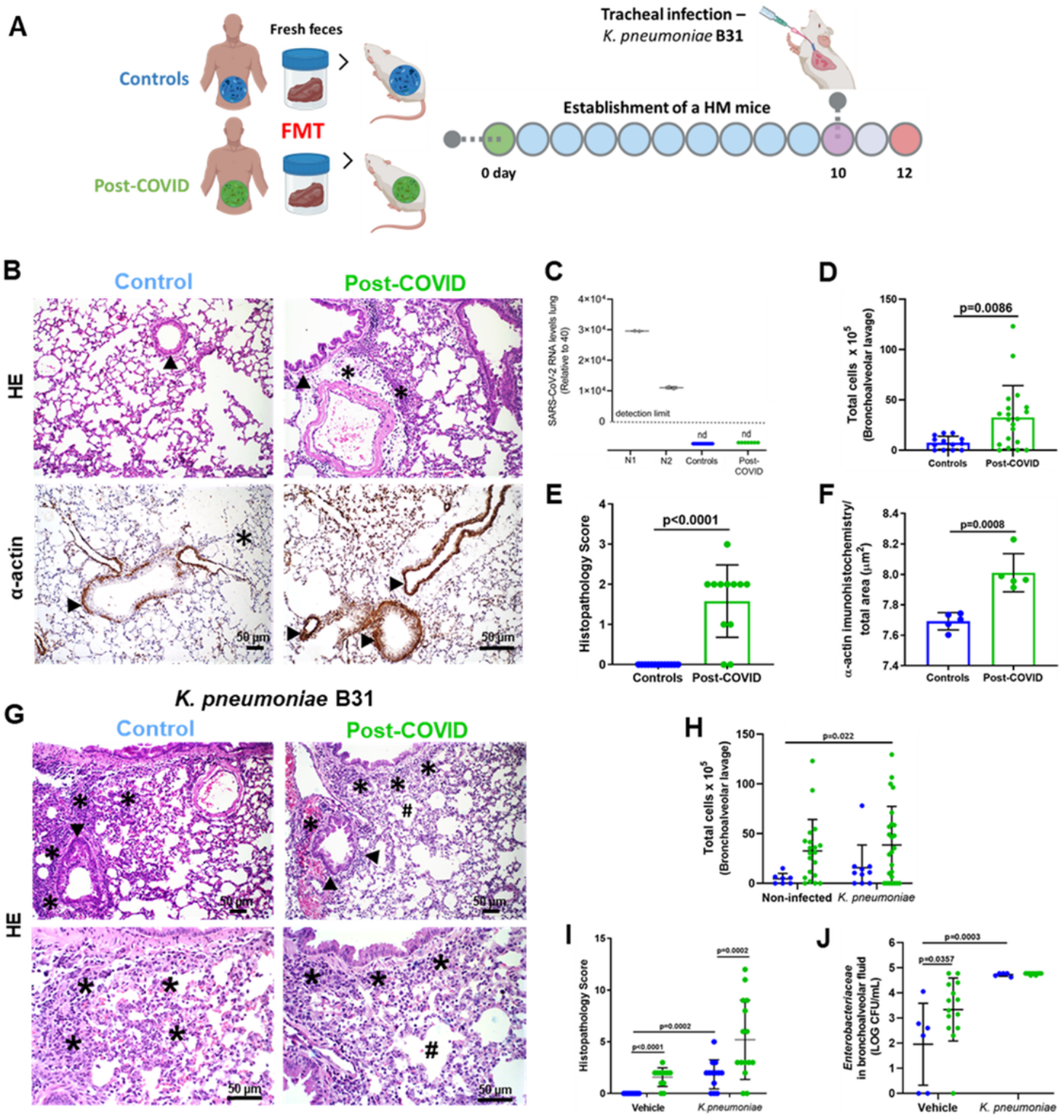

Figure 5

Impact of the Fecal Microbiota Transplant (FMT) in the gut-lung axis. **A** Graphical representation of the study design. **B** Histopathological aspects of the lung changes induced by FMT to GF mice. Lung samples from GF mice were immune-stained with anti-α-actin. Scale bar: 50µm. 20X objective. **C** RT-PCR

for SARS-CoV-2 in the lung of control and post-COVID mice. **D** Total number of cells in the BAL. **E** Histopathology score according to airways, vascular and parenchymal inflammation in controls and post-COVID-19 mice lungs. **F** Morphometrical analysis of muscular layer changes. Ten images of the muscular layer of each animal were acquired with a 40X objective. **G** Histopathological aspects of the lung changes induced by infection with *K. pneumoniae* B31. **H** Total number of cells in BAL by infection with *K. pneumoniae* B31. **I** Histopathology score according to airways, vascular and parenchymal inflammation in controls and post-COVID mice lungs induced by infection with *K. pneumoniae* B31. **J** Total number of cells in bronchoalveolar fluid of *Enterobacteriaceae*. Data are representative of two independent experiments. Statistical analysis: Student's *t*-test and Two-way ANOVA with Tukey's tests. Data are shown as mean and standard deviation (SD). Arrowheads indicate lung airways. Asterisks indicate inflammatory infiltrate. Sharp indicates the area of pulmonary emphysema. Number of families (N = 11). Each data point represents the FMT.

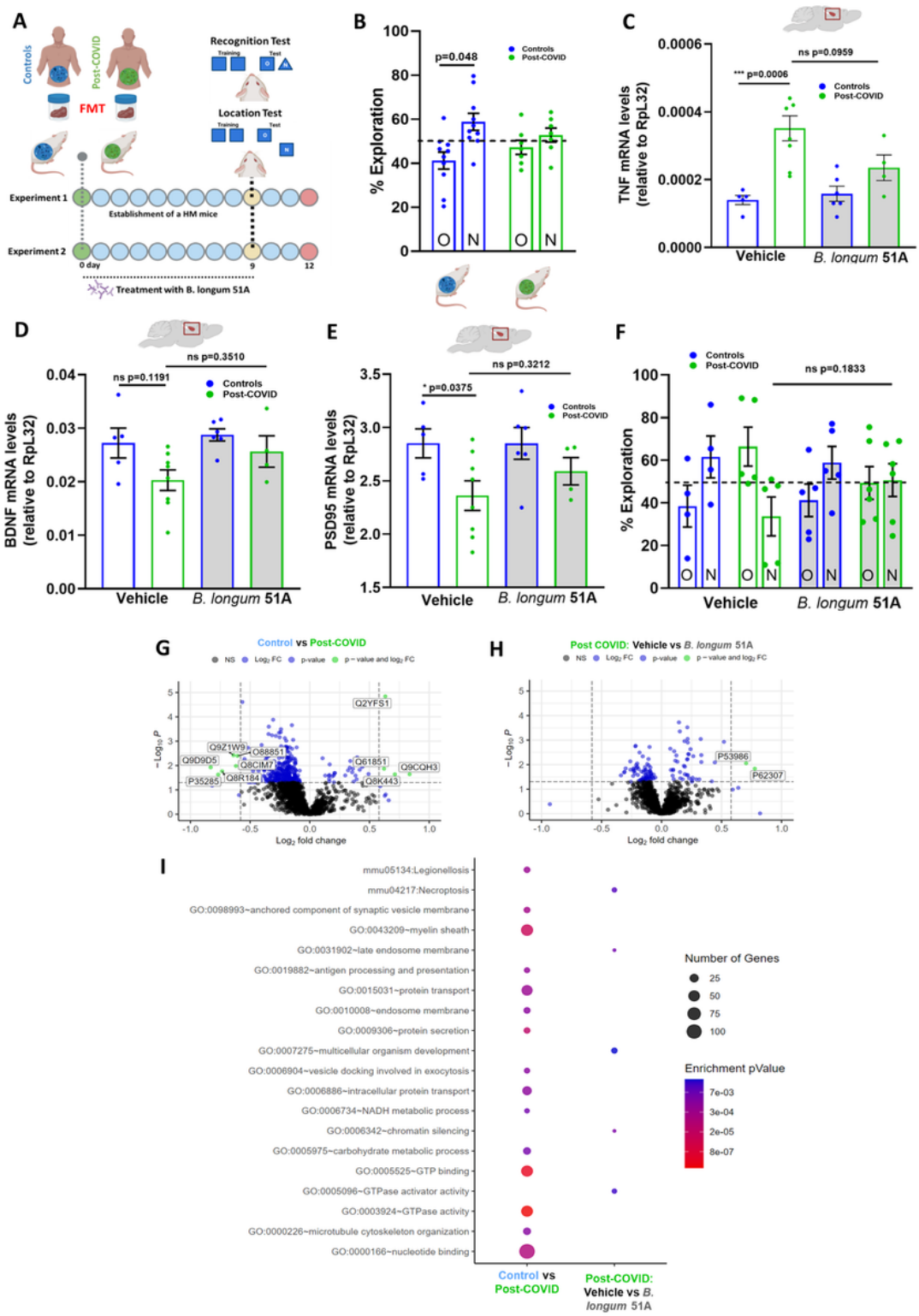

Figure 6

Impact of the post-COVID FMT and probiotic treatment in the gut-brain axis. **A** Graphical representation of the study design. GF mice received feces transfer obtained from control and post-COVID subjects' donors and vehicle or probiotic *B. longum* 5^{1A}, and thus, assessed to object location and recognition tests 9 days later. Additionally, following behavioral analysis, their hippocampus was submitted to gene expression and proteomic analysis. **B** GF mice that received post-COVID FMT showed memory impairment in the

object recognition and location tests. **C** Expression of TNFa, **D** BDNF, and **E** PSD95 mRNA levels in the hippocampus. **F** GF mice that received post-COVID FMT and treated with vehicle or *B. longum* 5^{1A} in the object recognition and location tests. **G** Volcano plots of differential expression according to proteome analysis of the hippocampus of mice that received control or post-COVID FMT **H** and post-COVID FMT and were treated with vehicle or *B. longum* 5^{1A}. **I** Pathways and ontology terms were obtained by enrichment analysis using the DAVID Bioinformatics Resources. Statistical analysis: one-sample t-test against the hypothetical value of 50% and Two-way ANOVA with Student-Newman-Keuls tests. Filtered tables were generated to exclude proteins with no statistical significance according to ANOVA ≥ 0.05. Data are shown as mean and standard deviation (SD). Number of families (N = 11). Each data point represents the FMT.

Supplementary Files

This is a list of supplementary files associated with this preprint. Click to download.

- AdditionalFile1FigureS1.pptx
- Additionalfile2TableS1.xlsx
- Additionalfile3TableS2.xlsx
- Additionalfile4TableS3.xls
- AdditionalFile5FigureS2.tiff
- AdditionalFile6FigureS3.tiff
- Additionalfile7TableS4.csv
- Additionalfile8TableS5.csv
- Additionalfile9TableS6.csv
- Additionalfile10TableS7.csv
- Additionalfile11FigureS4.tiff